

Thermal effects on ρ meson properties in an external magnetic field

Snigdha Ghosh^{a,c,*}, Arghya Mukherjee^{b,c,†}, Mahatsab Mandal^{d,‡}, Sourav Sarkar^{a,c,§} and Pradipt Roy^{b,c,¶}

^aVariable Energy Cyclotron Centre, 1/AF Bidhannagar, Kolkata 700 064, India

^bSaha Institute of Nuclear Physics, 1/AF Bidhannagar, Kolkata - 700064, India

^cHomi Bhabha National Institute, Training School Complex, Anushaktinagar, Mumbai - 400085, India and

^dGovernment General Degree College at Kalna-I, Burdwan, West Bengal - 713405, India

A detailed study of the analytic structure of 1-loop self energy graphs for neutral and charged ρ mesons is presented at finite temperature and arbitrary magnetic field using the real time formalism of thermal field theory. The imaginary part of the self energy is obtained from the discontinuities of these graphs across the Unitary and Landau cuts, which is seen to be different for ρ^0 and ρ^\pm . The magnetic field dependent vacuum contribution to the real part of the self energy, which is usually ignored, is found to be appreciable. A significant effect of temperature and magnetic field is seen in the self energy, spectral function, effective mass and dispersion relation of ρ^0 as well as of ρ^\pm relative to its trivial Landau shift. However, for charged ρ mesons, on account of the dominance of the Landau term, the effective mass appears to be independent of temperature. The trivial coupling of magnetic moment of ρ^\pm with external magnetic field, when incorporated in the calculation, makes the ρ^\pm to condense at high magnetic field.

I. INTRODUCTION

Recent researches in Quantum Chromodynamics(QCD) in presence of magnetic background have revealed many remarkable properties of strong interaction [1]. From anomalous Chiral Magnetic Effect (CME), Chiral Vortical Effect to Magnetic Catalysis(MC), Inverse Magnetic Catalysis(IMC) and vacuum superconductivity, these non-trivial interplay between the topology, symmetry and anomaly structure [2–9] have enriched the fundamental aspects of QCD to a great extent. On one hand, noticeable influence on the strongly interacting sector can be achieved only when the background magnetic field is strong enough to be comparable to QCD scale i.e $eB \approx m_\pi^2$, on the other hand, non-central heavy-ion collisions in Relativistic Heavy-Ion Collider(RHIC) and Large Hadron Collider(LHC) can generate magnetic fields of $eB \approx 15m_\pi^2$ [10]. Apart from its own theoretical intricacies, this promising platform for experimental manifestations has been one of the key reasons for ensuing interests in this field of research. Moreover, a similar environment inside the core of magnetars adds to its astrophysical and cosmological importance [11–18].

A large amount of progress has been achieved in solving the so called puzzle of MC and IMC using the effective models, most of which are focused on considering magnetic field dependent coupling constants or other magnetic field dependent parameters of the model (see for example [19]). One of the important methods for extracting the information of eB dependencies of the chiral phase transition parameters is to study the modifications of hadronic, in particular mesonic properties in presence of medium/density along with external magnetic field since they are more directly related to the chiral phase transition [20]. In this paper we mainly focus on the temperature modifications of ρ meson properties in presence of static homogeneous magnetic background. The study of the ρ meson properties like the effective mass and dispersion relations are important in the context of magnetic field induced vacuum superconductivity [9, 21–27]. It should be mentioned here that the dilepton production rate in heavy-ion collisions is directly proportional to the in-medium ρ spectral function and is well studied at vanishing magnetic field in Ref. [28–31]. However, the existence of such high external magnetic field in non central collisions does affect the spectral function of ρ [8, 32]. Thus the detailed study of the in-medium spectral properties of ρ meson in presence of eB may prove to be indispensable for analyzing the results of heavy-ion collision experiments.

Most of the calculations of one loop self energy functions at finite temperature under external magnetic field present in the literature employ either strong or weak magnetic field approximation [33–35]. A few of them have relaxed this approximation and calculations are presented for arbitrary value of magnetic field [36, 37]. In the later case, even though the full Schwinger propagator for the loop particles is considered, the real part of the self energy neglects

*Electronic address: snigdha.physics@gmail.com, snigdha@vecc.gov.in

†Electronic address: arghya.mukherjee@saha.ac.in

‡Electronic address: mahatsab@gmail.com

§Electronic address: sourav@vecc.gov.in

¶Electronic address: pradiptk.roy@saha.ac.in

the magnetic field dependent vacuum contribution. In this work we have taken the full Schwinger propagator for the loop particles and do not make any approximations on the magnitude of the magnetic field. We have also included the magnetic field dependent vacuum contributions to the real part of the self energy. In addition to these novelties, we have explicitly worked out the analytic structure of the self energy at finite temperature and non-zero magnetic field which to the best of our knowledge has not been discussed elsewhere. Discontinuities of the self energy graphs across the Unitary and Landau cut are seen to be different for the charged and neutral ρ mesons. It should be noted here that, if the external boson is charged, its momentum transverse to the external magnetic field is never zero due to Landau quantization. To show the importance of the loop correction of ρ^\pm at finite temperature and non-zero magnetic field, we first present various properties of ρ^\pm by neglecting this trivial Landau shift. Later, we also show results incorporating the Landau quantization of transverse momenta as well as including the trivial coupling of the magnetic moment of ρ^\pm with external magnetic field. In this case, we will show that the loop-correction to effective mass is subleading at all temperatures.

A few comments on the applicability of our calculation are in order. All the results in this paper, are presented for temperatures in the range $100 \text{ MeV} \leq T \leq 160 \text{ MeV}$ where, the degrees of freedom of strongly interacting matter are basically hadrons. However, if there exists a strong magnetic field (order of typical QCD scale), then the system may undergo a phase transition even in this temperature range (so called IMC effect [7]) to the deconfined phase where the degrees of freedom are quarks and gluons. In that case, the hadronic description will not be applicable. However, in this work we have not considered these possibilities.

The article is organized as follows. In Sec. II the vacuum self energy of ρ is discussed followed by the evaluation of the in-medium ρ self-energy at zero magnetic field in Sec. III. Next in Sec. IV, the in-medium self energy at non-zero external magnetic field is presented. Sec. V is devoted to the discussion of the analytic structure of the in-medium self energy functions in a magnetic field. In Sec. VI, the numerical results are shown and discussed. Finally we summarize and conclude in Sec. VII. Some of the relevant calculational details are provided in the Appendix.

II. ρ SELF ENERGY IN THE VACUUM

The lowest order (LO) Lagrangian for effective $\rho\pi\pi$ interaction is given by [31]

$$\mathcal{L}_{int} = -g_{\rho\pi\pi} \partial_\mu \vec{\rho}_\nu \cdot \partial^\mu \vec{\pi} \times \partial^\nu \vec{\pi},$$

with the effective coupling constant $g_{\rho\pi\pi} = 20.72 \text{ GeV}^{-2}$, which is fixed from the vacuum $\rho \rightarrow \pi\pi$ decay width $\Gamma_{\rho \rightarrow \pi\pi} = 150 \text{ MeV}$.

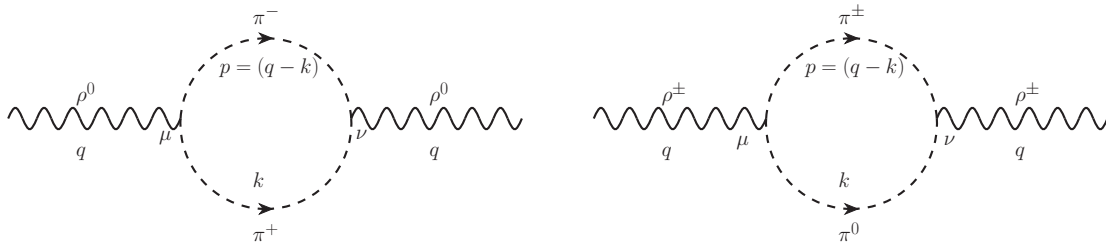


FIG. 1: Feynman diagrams for ρ self energy.

Using \mathcal{L}_{int} , the vacuum self energies of ρ^0 and ρ^\pm for Feynman diagrams shown in Fig. 1, can be written as

$$(\Pi_0^{\mu\nu}(q))_{vac} = i \int \frac{d^4k}{(2\pi)^4} \mathcal{N}^{\mu\nu}(q, k) \Delta_\pm(k) \Delta_\pm(p) \quad (1)$$

$$(\Pi_\pm^{\mu\nu}(q))_{vac} = i \int \frac{d^4k}{(2\pi)^4} \mathcal{N}^{\mu\nu}(q, k) \Delta_0(k) \Delta_\pm(p) \quad (2)$$

respectively. Here $\Delta_0(k) = \left(\frac{-1}{k^2 - m_0^2 + i\epsilon} \right)$ and $\Delta_\pm(k) = \left(\frac{-1}{k^2 - m_\pm^2 + i\epsilon} \right)$ are the vacuum Feynman propagators of π^0 and π^\pm with masses m_0 and m_\pm respectively and $\mathcal{N}^{\mu\nu}(q, k)$ is given by,

$$\mathcal{N}^{\mu\nu}(q, k) = g_{\rho\pi\pi}^2 [q^4 k^\mu k^\nu + (q \cdot k)^2 q^\mu q^\nu - q^2 (q \cdot k) (q^\mu k^\nu + k^\mu q^\nu)],$$

which contains the factors coming from the interaction vertices. The momentum integrations in Eqs. (1) and (2) can be evaluated using standard Feynman parametrization followed by dimensional regularization. If we take $m_0 = m_{\pm} = m_{\pi}$, then the vacuum self energies of ρ^0 and ρ^{\pm} are identical and is given by,

$$\Pi_{vac}^{\mu\nu}(q) = \left(\frac{q^2 g_{\rho\pi\pi}^2}{32\pi^2} \right) (q^2 g^{\mu\nu} - q^{\mu} q^{\nu}) \int_0^1 dx \Delta \left(\ln \frac{\Delta}{\mu_0} - 1 \right), \quad (3)$$

where $\Delta = m^2 - x(1-x)q^2 - i\epsilon$ and μ_0 is a scale of dimension GeV². The metric tensor in this work is taken as $g^{\mu\nu} = \text{diag}(1, -1, -1, -1)$.

III. ρ SELF ENERGY IN THE MEDIUM

In the real time formalism of thermal field theory, the thermal propagators as well as the self energies become 2×2 matrices [30, 38]. However, they can be diagonalized in terms of a single analytic function which is related to any one component of the corresponding 2×2 matrix, say the 11-component. The 11-component of the π^0 and π^{\pm} thermal propagators are given by,

$$\begin{aligned} D_0^{11}(k) &= \Delta_0(k) + 2i\eta^k \text{Im} \Delta_0(k) \\ D_{\pm}^{11}(k) &= \Delta_{\pm}(k) + 2i\eta^k \text{Im} \Delta_{\pm}(k) \end{aligned} \quad (4)$$

where, $\eta^k = [e^{k \cdot u/T} - 1]^{-1}$ is the Bose-Einstein distribution function of the pions with u^{μ} being the medium four-velocity. In local rest frame of the medium, $u^{\mu} \equiv (1, \vec{0})$. The complete in-medium propagator matrix $\mathbf{D}^{\mu\nu}$ satisfies the following Dyson-Schwinger equation,

$$\mathbf{D}^{\mu\nu} = \mathbf{\Delta}^{\mu\nu} - \mathbf{\Delta}^{\mu\alpha} \mathbf{\Pi}_{\alpha\beta} \mathbf{D}^{\beta\nu} \quad (6)$$

where, $\mathbf{\Delta}^{\mu\nu}$ is the free thermal vector propagator matrix and $\mathbf{\Pi}_{\alpha\beta}$ is the 1-loop thermal self energy matrix. Each of the quantities in Eq. (6) can be expressed in diagonal form in terms of analytic functions denoted by a bar, so that it can be written as,

$$\bar{\mathbf{D}}^{\mu\nu} = \bar{\mathbf{\Delta}}^{\mu\nu} - \bar{\mathbf{\Delta}}^{\mu\alpha} \bar{\mathbf{\Pi}}_{\alpha\beta} \bar{\mathbf{D}}^{\beta\nu}. \quad (7)$$

The self energy function $\bar{\mathbf{\Pi}}_{\alpha\beta}$ is related to the 11-component of $\mathbf{\Pi}_{\alpha\beta}$ by the following relations,

$$\text{Re} \bar{\mathbf{\Pi}}_{\alpha\beta}(q) = \text{Re} \Pi_{\alpha\beta}^{11}(q) \quad (8)$$

$$\text{Im} \bar{\mathbf{\Pi}}_{\alpha\beta}(q) = \epsilon(q^0) \tanh\left(\frac{q^0}{2T}\right) \text{Im} \Pi_{\alpha\beta}^{11} \quad (9)$$

where, $\epsilon(q^0) = \Theta(q^0) - \Theta(-q^0)$ is the sign function. In order to obtain the 11-component of the ρ^0 and ρ^{\pm} self energies, one has to replace the vacuum π^0 and π^{\pm} propagators in Eq. (1) and (2) by their corresponding 11-components as given in Eqs. (4) and (5),

$$(\Pi_0^{\mu\nu}(q))^{11} = i \int \frac{d^4 k}{(2\pi)^4} \mathcal{N}^{\mu\nu}(q, k) D_{\pm}^{11}(k) D_{\pm}^{11}(p) \quad (10)$$

$$(\Pi_{\pm}^{\mu\nu}(q))^{11} = i \int \frac{d^4 k}{(2\pi)^4} \mathcal{N}^{\mu\nu}(q, k) D_0^{11}(k) D_{\pm}^{11}(p). \quad (11)$$

Performing the k^0 integral and using Eqs. (8) and (9) we get the thermal self energy functions for ρ^0 and ρ^{\pm} which are identical if we take $m_0 = m_{\pm} = m_{\pi}$,

$$\begin{aligned} \text{Re} \bar{\mathbf{\Pi}}^{\mu\nu}(q) &= \text{Re} \Pi_{vac}^{\mu\nu}(q) + \int \frac{d^3 k}{(2\pi)^3} \frac{1}{2\omega_k \omega_p} \mathcal{P} \left[\left(\frac{\eta^k \omega_p \mathcal{N}^{\mu\nu}(k^0 = \omega_k)}{(q_0 - \omega_k)^2 - \omega_p^2} \right) + \left(\frac{\eta^k \omega_p \mathcal{N}^{\mu\nu}(k^0 = -\omega_k)}{(q_0 + \omega_k)^2 - \omega_p^2} \right) + \right. \\ &\quad \left. \left(\frac{\eta^p \omega_k \mathcal{N}^{\mu\nu}(k^0 = q_0 - \omega_p)}{(q_0 - \omega_p)^2 - \omega_k^2} \right) + \left(\frac{\eta^p \omega_k \mathcal{N}^{\mu\nu}(k^0 = q_0 + \omega_p)}{(q_0 + \omega_p)^2 - \omega_k^2} \right) \right] \end{aligned}$$

and

$$\begin{aligned} \text{Im } \bar{\Pi}^{\mu\nu}(q) = & -\pi\epsilon(q_0) \int \frac{d^3k}{(2\pi)^3} \frac{1}{4\omega_k\omega_p} \left[\mathcal{N}^{\mu\nu}(k^0 = \omega_k) \left\{ (1 + \eta^k + \eta^p)\delta(q_0 - \omega_k - \omega_p) + (-\eta^k + \eta^p)\delta(q_0 - \omega_k + \omega_p) \right\} \right. \\ & \left. + \mathcal{N}^{\mu\nu}(k^0 = -\omega_k) \left\{ (-1 - \eta^k - \eta^p)\delta(q_0 + \omega_k + \omega_p) + (\eta^k - \eta^p)\delta(q_0 + \omega_k - \omega_p) \right\} \right], \quad (12) \end{aligned}$$

where, $\omega_k = \sqrt{\vec{k}^2 + m_\pi^2}$, $\omega_p = \sqrt{\vec{p}^2 + m_\pi^2} = \sqrt{(\vec{q} - \vec{k})^2 + m_\pi^2}$ and \mathcal{P} denotes the Cauchy principal value integration.

IV. ρ SELF ENERGY IN THE MEDIUM UNDER EXTERNAL MAGNETIC FIELD

In presence of external magnetic field (in addition to finite temperature), the π^0 propagator remains unaffected whereas the 11-component of π^\pm propagator becomes [36],

$$D_B^{11}(k) = \Delta_B(k) + 2i\eta^k \text{Im } \Delta_B(k),$$

where, $\Delta_B(k)$ is the Schwinger proper time propagator for a charged scalar field [34, 39] in momentum space,

$$\Delta_B(k) = i \int_0^\infty \frac{ds}{\cos(eBs)} \exp \left[is \left(k_\parallel^2 + k_\perp^2 \frac{\tan(eBs)}{eBs} - m_\pi^2 + i\epsilon \right) \right]. \quad (13)$$

The corresponding coordinate space propagator contains a phase factor which is not translationally invariant. However with a suitable choice of the gauge, the phase factor can be removed [40], and one can work with the momentum space propagator. In Eq. (13), $e = |e|$ is the absolute electronic charge; the external magnetic field is taken along the +ve z-direction ($\vec{B} = B\hat{z}$) and correspondingly any four-vector a is decomposed as $a = (a_\parallel + a_\perp)$, where $a_\parallel^\mu \equiv (a^0, 0, 0, a_z)$ and $a_\perp^\mu \equiv (0, a_x, a_y, 0)$. The metric tensor $g^{\mu\nu}$ is also decomposed as $g^{\mu\nu} = g_\parallel^{\mu\nu} + g_\perp^{\mu\nu}$, where $g_\parallel^{\mu\nu} = \text{diag}(1, 0, 0, -1)$ and $g_\perp^{\mu\nu} = \text{diag}(0, -1, -1, 0)$. Performing the proper time integration in Eq. (13), one gets,

$$\Delta_B(k) = \sum_{l=0}^{\infty} \frac{-\phi_l(\alpha_k)}{k_\parallel^2 - m_l^2 + i\epsilon},$$

where

$$m_l = \sqrt{m_\pi^2 + (2l + 1)eB}, \quad (14)$$

$\phi_l(\alpha_k) = 2(-1)^l L_l(2\alpha_k)e^{-\alpha_k}$, $\alpha_k = -k_\perp^2/eB$ and $L_l(x)$ is the Laguerre polynomial of order l with $L_{-1}(x) = 0$. Replacing $D_\pm^{11} \rightarrow D_B^{11}$ in Eqs. (10) and (11), and following Eqs. (8) and (9), one gets the ρ^0 and ρ^\pm self energy functions at finite temperature in external magnetic field as,

$$\bar{\Pi}_0^{\mu\nu} = (\Pi_0^{\mu\nu})_B + (\Pi_0^{\mu\nu})_{BT} \quad (15)$$

$$\bar{\Pi}_\pm^{\mu\nu} = (\Pi_\pm^{\mu\nu})_B + (\Pi_\pm^{\mu\nu})_{BT}. \quad (16)$$

In Eqs. (15) and (16), subscript “ B ” and “ BT ” denote purely magnetic field dependent and both magnetic field as well as temperature dependent contributions respectively.

It is well known that the momenta of charged bosons transverse to the direction of external magnetic field are Landau quantized so that $q_\perp^2 = -(2n + 1)eB$ with $n = 0, 1, 2, \dots$. So for ρ^\pm , we present results for arbitrary four-momentum $q^\mu \equiv (q^0, q_x, q_y, q_z)$, whereas for ρ^0 we take for simplicity $q^\mu \equiv (q^0, 0, 0, q_z)$. The calculations of the real parts of the “ B ” terms i.e. the magnetic field dependent vacuum contributions are rather involved for which some relevant intermediate steps are provided in the Appendices (A) and (B). In comparison, the calculations of the real parts of the “ BT ” terms as well as the imaginary parts of the self energies are relatively straight forward and similar to the $eB = 0$ case. We summarize the explicit forms of different terms in Eqs. (15) and (16) below. The expressions for the real parts of ρ^0 self energy function are

$$\begin{aligned} \text{Re}(\Pi_0^{\mu\nu}(q^0, q_z))_B = & \text{Re } \Pi_{vac}^{\mu\nu} + \left(\frac{g_{\rho\pi\pi}^2 q_\parallel^2}{32\pi^2} \right) \int_0^1 dx \left[(q_\parallel^2 g_\parallel^{\mu\nu} - q_\parallel^\mu q_\parallel^\nu) \text{Re} \left(2eB \ln \Gamma \left(\frac{\Delta}{2eB} + \frac{1}{2} \right) - \Delta \ln \frac{\Delta}{2eB} + \Delta \right) \right. \\ & \left. + q_\parallel^2 g_\perp^{\mu\nu} \text{Re} \left(\frac{\Delta}{2} \Psi \left(\frac{\Delta}{2eB} + \frac{1}{2} \right) + \frac{1}{2} (\Delta + (2x - 1)eB) \Psi \left(\frac{\Delta}{2eB} + \frac{1}{2} + x \right) - \Delta \ln \frac{\Delta}{2eB} \right) \right] \quad (17) \end{aligned}$$

$$\text{Re}(\Pi_0^{\mu\nu}(q^0, q_z))_{BT} = \sum_{l=0}^{\infty} \sum_{n=0}^{\infty} \int_{-\infty}^{\infty} \frac{dk_z}{2\pi} \frac{1}{2\omega_k^l \omega_p^n} \mathcal{P} \left[\left(\frac{\eta_l^k \omega_p^n \mathcal{N}_{nl}^{\mu\nu}(k^0 = \omega_k^l)}{(q_0 - \omega_k^l)^2 - (\omega_p^n)^2} \right) + \left(\frac{\eta_l^k \omega_p^n \mathcal{N}_{nl}^{\mu\nu}(k^0 = -\omega_k^l)}{(q_0 + \omega_k^l)^2 - (\omega_p^n)^2} \right) + \right. \\ \left. \left(\frac{\eta_n^p \omega_k^l \mathcal{N}_{nl}^{\mu\nu}(k^0 = q_0 - \omega_p^n)}{(q_0 - \omega_p^n)^2 - (\omega_k^l)^2} \right) + \left(\frac{\eta_n^p \omega_k^l \mathcal{N}_{nl}^{\mu\nu}(k^0 = q_0 + \omega_p^n)}{(q_0 + \omega_p^n)^2 - (\omega_k^l)^2} \right) \right],$$

while the imaginary part is

$$\text{Im} \bar{\Pi}_0^{\mu\nu}(q^0, q_z) = -\pi\epsilon(q_0) \sum_{l=0}^{\infty} \sum_{n=0}^{\infty} \int_{-\infty}^{\infty} \frac{dk_z}{2\pi} \frac{1}{4\omega_k^l \omega_p^n} \times \\ \left[\mathcal{N}_{nl}^{\mu\nu}(k^0 = \omega_k^l) \left\{ (1 + \eta_l^k + \eta_n^p) \delta(q_0 - \omega_k^l - \omega_p^n) + (-\eta_l^k + \eta_n^p) \delta(q_0 - \omega_k^l + \omega_p^n) \right\} \right. \\ \left. + \mathcal{N}_{nl}^{\mu\nu}(k^0 = -\omega_k^l) \left\{ (-1 - \eta_l^k - \eta_n^p) \delta(q_0 + \omega_k^l + \omega_p^n) + (\eta_l^k - \eta_n^p) \delta(q_0 + \omega_k^l - \omega_p^n) \right\} \right]. \quad (18)$$

For the charged ρ meson, the corresponding expressions are:

$$\text{Re}(\Pi_{\pm}^{\mu\nu}(q^0, \vec{q}))_B = \text{Re} \Pi_{vac}^{\mu\nu} + \left(\frac{g_{\rho\pi\pi}^2}{32\pi^2} \right) \int_0^1 \int_0^1 dx dz z^{\Delta/m_\pi^2 - 1} \left[z^{-y(1-x)q_\perp^2/m_\pi^2} \left(\frac{1}{\zeta} \right) \text{sech} \left(x \frac{eB}{m_\pi^2} \ln z \right) \right. \\ \left. \left(\frac{P^{\mu\nu}}{\ln z} + \frac{2Q^{\mu\nu}}{m_\pi^2} + \frac{R^{\mu\nu}}{\zeta m_\pi^2} \right) - z^{-x(1-x)q_\perp^2/m_\pi^2} \left(\frac{m_\pi^2 q^2}{(\ln z)^2} \right) (q^2 g^{\mu\nu} - q^\mu q^\nu) \right] \quad (19)$$

and

$$\text{Re}(\Pi_{\pm}^{\mu\nu}(q^0, \vec{q}))_{BT} = \sum_{n=0}^{\infty} \int \frac{d^3 k}{(2\pi)^3} \frac{\phi_n(\alpha_p)}{2\omega_k \omega_p^n} \mathcal{P} \left[\left(\frac{\eta^k \omega_p^n \mathcal{N}^{\mu\nu}(k^0 = \omega_k)}{(q_0 - \omega_k)^2 - (\omega_p^n)^2} \right) + \left(\frac{\eta^k \omega_p^n \mathcal{N}^{\mu\nu}(k^0 = -\omega_k)}{(q_0 + \omega_k)^2 - (\omega_p^n)^2} \right) + \right. \\ \left. \left(\frac{\eta_n^p \omega_k \mathcal{N}^{\mu\nu}(k^0 = q_0 - \omega_p^n)}{(q_0 - \omega_p^n)^2 - (\omega_k)^2} \right) + \left(\frac{\eta_n^p \omega_k \mathcal{N}^{\mu\nu}(k^0 = q_0 + \omega_p^n)}{(q_0 + \omega_p^n)^2 - (\omega_k)^2} \right) \right] \\ \text{Im} \bar{\Pi}_{\pm}^{\mu\nu}(q^0, \vec{q}) = -\pi\epsilon(q_0) \sum_{n=0}^{\infty} \int \frac{d^3 k}{(2\pi)^3} \frac{\phi_n(\alpha_p)}{4\omega_k \omega_p^n} \times \\ \left[\mathcal{N}^{\mu\nu}(k^0 = \omega_k) \left\{ (1 + \eta^k + \eta_n^p) \delta(q_0 - \omega_k - \omega_p^n) + (-\eta^k + \eta_n^p) \delta(q_0 - \omega_k + \omega_p^n) \right\} \right. \\ \left. + \mathcal{N}^{\mu\nu}(k^0 = -\omega_k) \left\{ (-1 - \eta^k - \eta_n^p) \delta(q_0 + \omega_k + \omega_p^n) + (\eta^k - \eta_n^p) \delta(q_0 + \omega_k - \omega_p^n) \right\} \right], \quad (20)$$

where, $\Psi(z)$ is the digamma function, $\tilde{\zeta} = (1-x)\frac{1}{m_\pi^2} \ln z + \frac{1}{eB} \tanh\left(x\frac{eB}{m_\pi^2} \ln z\right)$, $y = \frac{1}{\zeta eB} \tanh\left(x\frac{eB}{m_\pi^2} \ln z\right)$, $\omega_k^l = \sqrt{k_z^2 + m_l^2}$, $\eta_k^l = \left[e^{\omega_k^l/T} - 1\right]^{-1}$ and

$$\mathcal{N}_{nl}^{\mu\nu}(q_{\parallel}, k_{\parallel}) = \frac{g_{\rho\pi\pi}^2}{2} (-1)^{n+l} \left(\frac{eB}{\pi} \right) \left[\left\{ q_{\parallel}^4 k_{\parallel}^{\mu} k_{\parallel}^{\nu} + (q_{\parallel} \cdot k_{\parallel})^2 q_{\parallel}^{\mu} q_{\parallel}^{\nu} - q_{\parallel}^2 (q_{\parallel} \cdot k_{\parallel}) (q_{\parallel}^{\mu} k_{\parallel}^{\nu} + k_{\parallel}^{\mu} q_{\parallel}^{\nu}) \right\} \delta_{n,l} \right. \\ \left. - \frac{eB}{4} q_{\parallel}^4 g_{\perp}^{\mu\nu} \left\{ (2n+1)\delta_{n,l} - n\delta_{n-1,l} - (n+1)\delta_{n+1,l} \right\} \right]. \quad (21)$$

The expressions for $P^{\mu\nu}$, $Q^{\mu\nu}$ and $R^{\mu\nu}$ are provided in Appendix (B).

V. ANALYTIC STRUCTURE OF THE IMAGINARY PARTS

Each of the imaginary parts of the self energy functions in Eqs. (12), (18) and (20) contains four Dirac delta functions which will give rise to branch cuts of the self energy function in the complex q^0 plane, details of which

are provided in Appendix C. Let us first discuss the analytic structure at finite temperature in absence of magnetic field. In Eq. (12), the first term containing $\delta(q^0 - \omega_k - \omega_p)$ is non vanishing for $\sqrt{\vec{q}^2 + 4m_\pi^2} < q^0 < \infty$ and we call this ‘‘Unitary-I’’ cut. The second term containing $\delta(q^0 - \omega_k + \omega_p)$ is non vanishing for $-|\vec{q}| < q^0 < 0$ and this is the ‘‘Landau-II’’ cut. The third term containing $\delta(q^0 + \omega_k + \omega_p)$ is non vanishing for $-\infty < q^0 < -\sqrt{\vec{q}^2 + 4m_\pi^2}$ and we call this is ‘‘Unitary-II’’ cut. Finally the fourth term containing $\delta(q^0 + \omega_k - \omega_p)$ is non vanishing for $0 < q^0 < |\vec{q}|$ and this is the ‘‘Landau-I’’ cut. These different cuts are shown in Fig. 2 and correspond to different physical processes. We are interested in the physical kinematic region $q^0 > 0$ and $q^2 > 0$. In this region Unitary-I and Landau-I terms contribute. Unitary-I cut corresponds to the decay of a ρ into two pions which can also happen in vacuum, whereas the Landau-I cut is purely a medium effect which corresponds to the absorption of a ρ due to scattering with a π producing a π in the final state. If we take $\vec{q} = \vec{0}$, then the Landau contributions will be absent and we are left with only Unitary cut contributions.

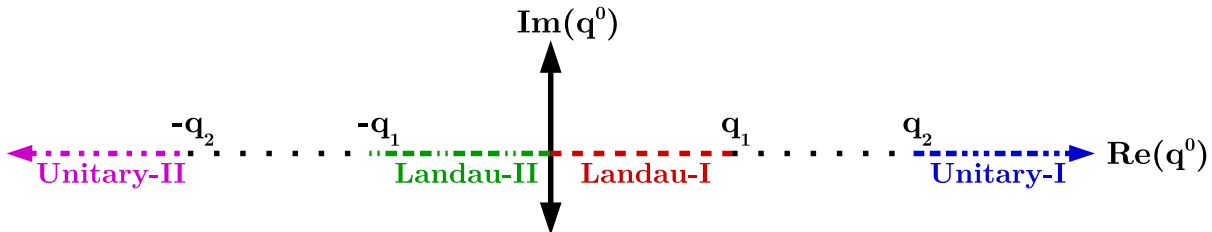


FIG. 2: Different branch cuts of the in-medium self energy function of the ρ at zero magnetic field in the complex q^0 plane for a given \vec{q} . The points correspond to $q_1 = |\vec{q}|$ and $q_2 = \sqrt{\vec{q}^2 + 4m_\pi^2}$.

Let us now turn on the magnetic field. The imaginary part of ρ^0 self energy function in presence of the external magnetic field in Eq. (18) is non vanishing at four different kinematic regions. Note that in this case the quantity m_l in Eq. (14) for charged pions in the loop contains a contribution from the transverse momentum component which are quantized. As shown in Appendix C, the Unitary-I and Unitary-II cuts are defined in $\sqrt{q_z^2 + 4(m_\pi^2 + eB)} < q^0 < \infty$ and $-\infty < q^0 < -\sqrt{q_z^2 + 4(m_\pi^2 + eB)}$ respectively, whereas both the Landau-I and Landau-II cuts are defined in $|q^0| < \sqrt{q_z^2 + (\sqrt{m_\pi^2 + eB} - \sqrt{m_\pi^2 + 3eB})^2}$. These cuts are shown in Fig. 3. It is to be noted that, in presence of the external magnetic field, the in-medium ρ^0 self energy always possesses the Landau contribution even if $\vec{q} = \vec{0}$.

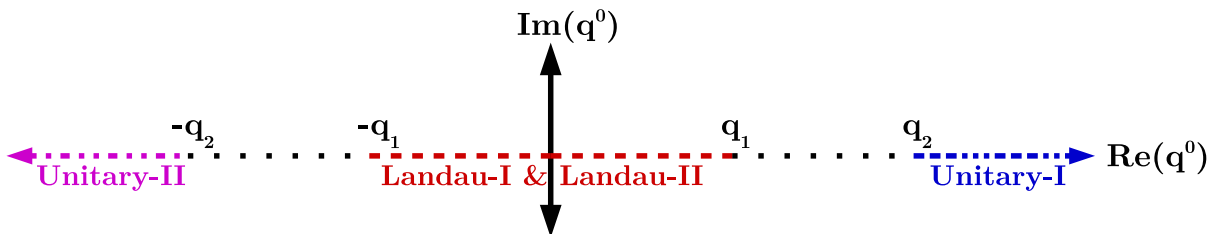


FIG. 3: Different branch cuts of the in-medium self energy function of the ρ^0 under external magnetic field in the complex q^0 plane for a given \vec{q} . The points correspond to $q_1 = \sqrt{q_z^2 + (\sqrt{m_\pi^2 + eB} - \sqrt{m_\pi^2 + 3eB})^2}$ and $q_2 = \sqrt{q_z^2 + 4(m_\pi^2 + eB)}$.

In a similar way, the imaginary part of ρ^\pm self energy function in presence of the external magnetic field in Eq. (20) has its Unitary-I and Unitary-II cuts in the kinematic domain $\sqrt{q_z^2 + (\sqrt{m_\pi^2 + eB} + m_\pi)^2} < q^0 < \infty$ and $-\infty < q^0 < -\sqrt{q_z^2 + (\sqrt{m_\pi^2 + eB} + m_\pi)^2}$ respectively, whereas it has its Landau-I and Landau-II cuts in the kinematic domain $0 < q^0 < \infty$ and $-\infty < q^0 < 0$ respectively. These cuts are displayed in Fig. 4. In this case also the in-medium ρ^\pm self energy always has a finite Landau cut contribution even if $\vec{q} = \vec{0}$.

The imaginary parts given in Eq. (12),(18) and (20) have been further simplified using the Dirac delta functions present in the integrand. For the sake of simplicity in analytic calculations Eq. (12) and (18) are simplified by taking $\vec{q} = \vec{0}$. However, for Eq. (20), we have taken $\vec{q} = (q_x, q_y, 0)$. The simplified form of the imaginary parts can be

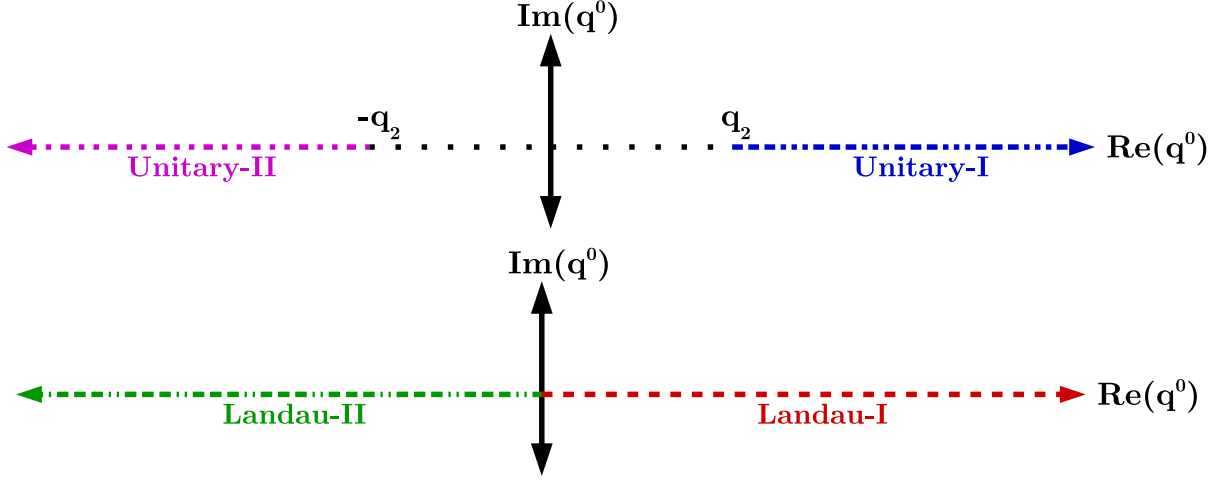


FIG. 4: Different branch cuts of the in-medium self energy functions of the ρ^\pm under external magnetic field in the complex q^0 plane for a given \vec{q} . Upper-Panel shows the Unitary cut regions with $q_2 = \sqrt{q_z^2 + (\sqrt{m_\pi^2 + eB} + m_\pi)^2}$. Lower-Panel shows the Landau cut regions.

obtained from Appendix (D),

$$\text{Im } \bar{\Pi}^{\mu\nu}(q^0, \vec{q} = \vec{0}) = \left(\frac{-\epsilon(q^0)\tilde{k}}{8\pi q^0} \right) \left[U_1(q^0, |\vec{k}| = \tilde{k}) \Theta(q^0 - 2m_\pi) + U_2(q^0, |\vec{k}| = \tilde{k}) \Theta(-q^0 - 2m_\pi) \right] \quad (22)$$

$$\begin{aligned} \text{Im } \bar{\Pi}_0^{\mu\nu}(q^0, \vec{q} = \vec{0}) = & \left(\frac{-\epsilon(q^0)}{4|q^0|} \right) \sum_{l=0}^{\infty} \sum_{n=0}^{\infty} \frac{1}{\tilde{k}_z} \left[U_1^{n,l}(q^0, \tilde{k}_z) \Theta(q^0 - m_l - m_n) + U_2^{n,l}(q^0, \tilde{k}_z) \Theta(-q^0 - m_l - m_n) \right. \\ & + L_1^{n,l}(q^0, \tilde{k}_z) \Theta\{-q^0 - \min(m_l - m_n, 0)\} \Theta\{\max(m_l - m_n, 0) + q^0\} \\ & \left. + L_2^{n,l}(q^0, \tilde{k}_z) \Theta\{q^0 - \min(m_l - m_n, 0)\} \Theta\{\max(m_l - m_n, 0) - q^0\} \right] \quad (23) \end{aligned}$$

$$\begin{aligned} \text{Im } \bar{\Pi}_\pm^{\mu\nu}(q^0, q_x, q_y) = & \left(\frac{-\epsilon(q^0)}{32\pi^2} \right) \sum_{n=0}^{\infty} \int_0^{2\pi} d\phi \left[\int_{\omega_-}^{\omega_0} \frac{d\omega_k}{|\vec{k}| \cos \theta_0} \left\{ U_1^n(q^0, |\vec{k}|, \theta_0, \phi) + U_1^n(q^0, |\vec{k}|, -\theta_0, \phi) \right\} \Theta(q^0 - m_\pi - m_n) \right. \\ & + \int_{-\omega_+}^{-\omega_0} \frac{d\omega_k}{|\vec{k}| \cos \theta'_0} \left\{ U_2^n(q^0, |\vec{k}|, \theta'_0, \phi) + U_2^n(q^0, |\vec{k}|, -\theta'_0, \phi) \right\} \Theta(-q^0 - m_\pi - m_n) \\ & + \int_{-\omega_0}^{-\omega_-} \frac{d\omega_k}{|\vec{k}| \cos \theta'_0} \left\{ L_1^n(q^0, |\vec{k}|, \theta'_0, \phi) + L_1^n(q^0, |\vec{k}|, -\theta'_0, \phi) \right\} \Theta(-q^0 - m_\pi + m_n) \Theta(q^0) \\ & \left. + \int_{\omega_0}^{-\omega_+} \frac{d\omega_k}{|\vec{k}| \cos \theta_0} \left\{ L_2^n(q^0, |\vec{k}|, \theta_0, \phi) + L_2^n(q^0, |\vec{k}|, -\theta_0, \phi) \right\} \Theta(q^0 - m_\pi + m_n) \Theta(-q^0) \right] \quad (24) \end{aligned}$$

where, $\tilde{k}_z = \frac{1}{2q^0} \lambda^{1/2} (q_0^2, m_l^2, m_n^2)$, $\omega_\pm = (q^0 \pm m_n)$ and $\omega_0 = \frac{1}{2q^0} (q_0^2 + m_\pi^2 - m_n^2)$. The Lorentz indices μ, ν are contained in $U_{1,2}$ and $L_{1,2}$ (see Appendix D).

VI. NUMERICAL RESULTS

We begin this section by showing the imaginary and real parts of the in-medium self energy function of ρ meson under external magnetic field. We will present numerical results for the spin averaged quantity

$$\Pi_{0,\pm} = \frac{1}{3} g_{\mu\nu} \bar{\Pi}_{0,\pm}^{\mu\nu}. \quad (25)$$

First, we have checked numerically that in the limit $eB \rightarrow 0$, the $eB = 0$ results ($T \neq 0$) are exactly reproduced, i.e.

$$\lim_{eB \rightarrow 0} \bar{\Pi}_0^{\mu\nu} = \lim_{eB \rightarrow 0} \bar{\Pi}_{\pm}^{\mu\nu} = \bar{\Pi}^{\mu\nu}.$$

To take $eB \rightarrow 0$ limit, numerically we have taken upto 300 Landau levels for a convergent result. However, for the other results presented here for $eB \geq 0.05 \text{ GeV}^2$, the results are well convergent with 200 Landau levels.

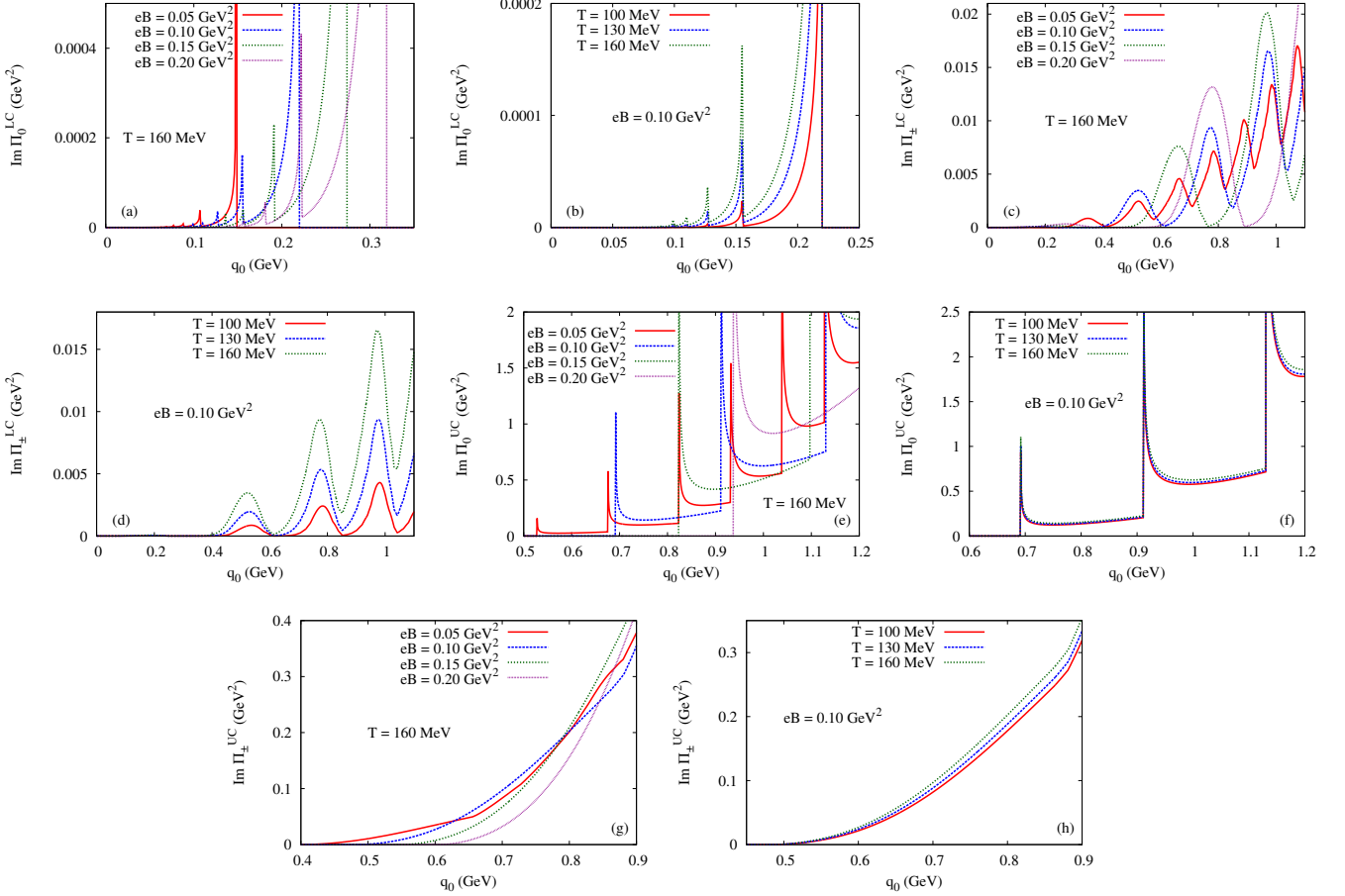


FIG. 5: The Landau cut and Unitary cut contributions to the imaginary part of the self energy function of rho meson. (a) Landau cut for ρ^0 (c) Landau cut for ρ^\pm (e) Unitary cut for ρ^0 (f) Unitary cut for ρ^\pm , are shown at constant temperature (160 MeV) and at different values of the magnetic field (0.05, 0.10, 0.15 and 0.20 GeV^2 respectively). (b) Landau cut for ρ^0 (d) Landau cut for ρ^\pm (f) Unitary cut for ρ^0 (h) Unitary cut for ρ^\pm , are shown at constant magnetic field (0.01 GeV^2) and at different values of the temperature (100, 130 and 160 MeV respectively).

We have taken the neutral as well as charged rho meson three momenta to be zero in Figures 5 - 9. In Fig. 5(a)-(d), the Landau cut contributions for the imaginary parts of the self energy functions are shown. The spikes occurring in Fig. 5(a) and (b) for the ρ^0 are due to the “Threshold Singularity” for each Landau level as can be understood from Eq. (23). In this equation the \tilde{k}_z present in the denominator has appeared due to dimensional reduction in the ρ^0 self energy. For a particular set of Landau levels $\{n, l\}$, we have

$$\tilde{k}_z = \frac{1}{2q^0} \lambda^{1/2} (q_0^2, m_l^2, m_n^2) = \frac{1}{2q^0} (q^0 + m_l + m_n) (q^0 - m_l - m_n) (q^0 + m_l - m_n) (q^0 - m_l - m_n),$$

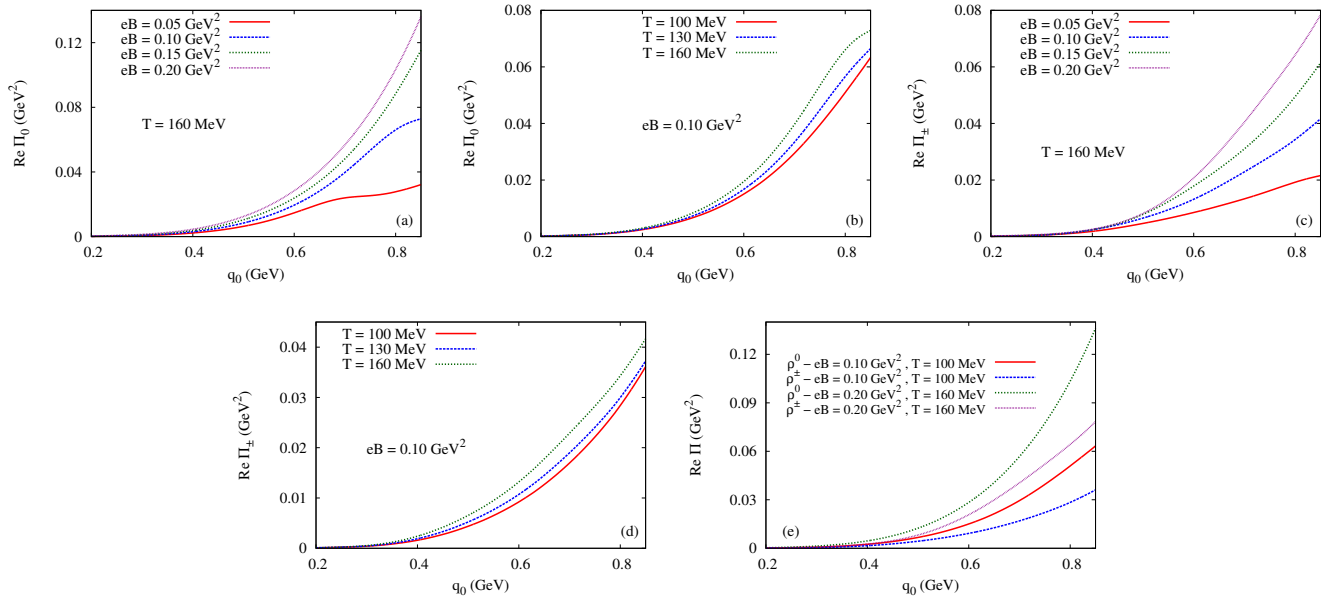


FIG. 6: The real part of the self energy function of (a) ρ^0 (c) ρ^\pm , at constant temperature (160 MeV) and at different values of the magnetic field (0.05, 0.10, 0.15 and 0.20 GeV^2 respectively). The real part of the self energy function of (b) ρ^0 (d) ρ^\pm , at constant magnetic field (0.01 GeV^2) and at different values of the temperature (100, 130 and 160 MeV) respectively. (e) The comparison of the real part of the self energy function between ρ^0 and ρ^\pm at two different combinations of the magnetic field and temperature ($eB=0.10 \text{ GeV}^2$, $T=100 \text{ MeV}$ and $eB=0.20 \text{ GeV}^2$, $T=160 \text{ MeV}$ respectively).

which will go to zero at each threshold of Unitary and Landau cut defined in terms of the step functions in Eq. (23) which gives rise to the spike like structure in the upper panel. Physically, the spikes correspond to the fluctuation of ρ^0 into two pions occurring in the transverse plane with respect to the direction of external magnetic field. Moreover, at these threshold values of q^0 , the ρ^0 will be (infinitely) unstable and will decay into pions immediately. In Fig. 5(a) we have shown results for four different values of eB (0.05, 0.10, 0.15 and 0.20 GeV^2 respectively) at a constant temperature 160 MeV. As eB increases, the thresholds of the Landau cuts move towards higher values of q^0 as evident from Eq. (23). Also with the increase of eB , the separation among the spikes becomes larger. In Fig. 5(b), results are shown at a constant eB (0.10 GeV^2) at three different values of temperature (100, 130 and 160 MeV respectively). In this case the threshold remains unchanged but the magnitude becomes larger which is due to the increase of the magnitude of thermal distribution functions with the increase of temperature.

In Fig. 5(c)-(d), similar results for the ρ^\pm are shown. In this case, there is no threshold for the Landau cuts and they extend from $-\infty < q^0 < \infty$. The oscillations are due to the presence of a Laguerre polynomial in Eq. (24). It is also to be noted that, at a larger value of eB the significant contributions start from a higher q^0 . In Fig. 5(d), we see that the magnitude of the imaginary parts increases with the increase in temperature keeping the overall structure unaltered which is again due to increase in the thermal distribution function with the increase of temperature.

In Fig. 5(e)-(h) the Unitary cut contributions to the imaginary part of the self energy functions are presented. In Fig. 5(e), results for ρ^0 at a constant temperature (160 MeV) and at four different values of the magnetic field (0.05, 0.10, 0.15 and 0.20 GeV^2 respectively) are shown. Similar to the Landau cut contribution, the Unitary cut contributions of ρ^0 also suffer from the "Threshold Singularities". As the magnetic field increases, the thresholds of the Unitary cuts move towards higher q^0 and the separations among the spikes increase. In Fig. 5(f), results are shown for a constant eB (0.10 GeV^2) and at three different values of the temperature (100, 130 and 160 MeV respectively). As the temperature increases, the magnitudes of the self energies increase keeping the thresholds unchanged similar to the Landau cut contributions. However, unlike the Landau contributions, the Unitary contributions are dominated by the vacuum contribution and the effect of increase of temperature is rather small.

In Fig. 5(g)-(h), results are presented for the charged ρ . The ρ^\pm has different thresholds for the Unitary cuts than the ρ^0 as given in Eq. (24). The displacement of the Unitary cut threshold towards higher q^0 with the increase in eB is smaller compared to that of ρ^0 and this will have significant effect on the spectral functions. Small oscillations can be noticed in the graphs, which are due to the presence of a Laguerre polynomial. However these oscillations and the effect of temperature is not of much significance as the Unitary cut is dominated by the vacuum contributions.

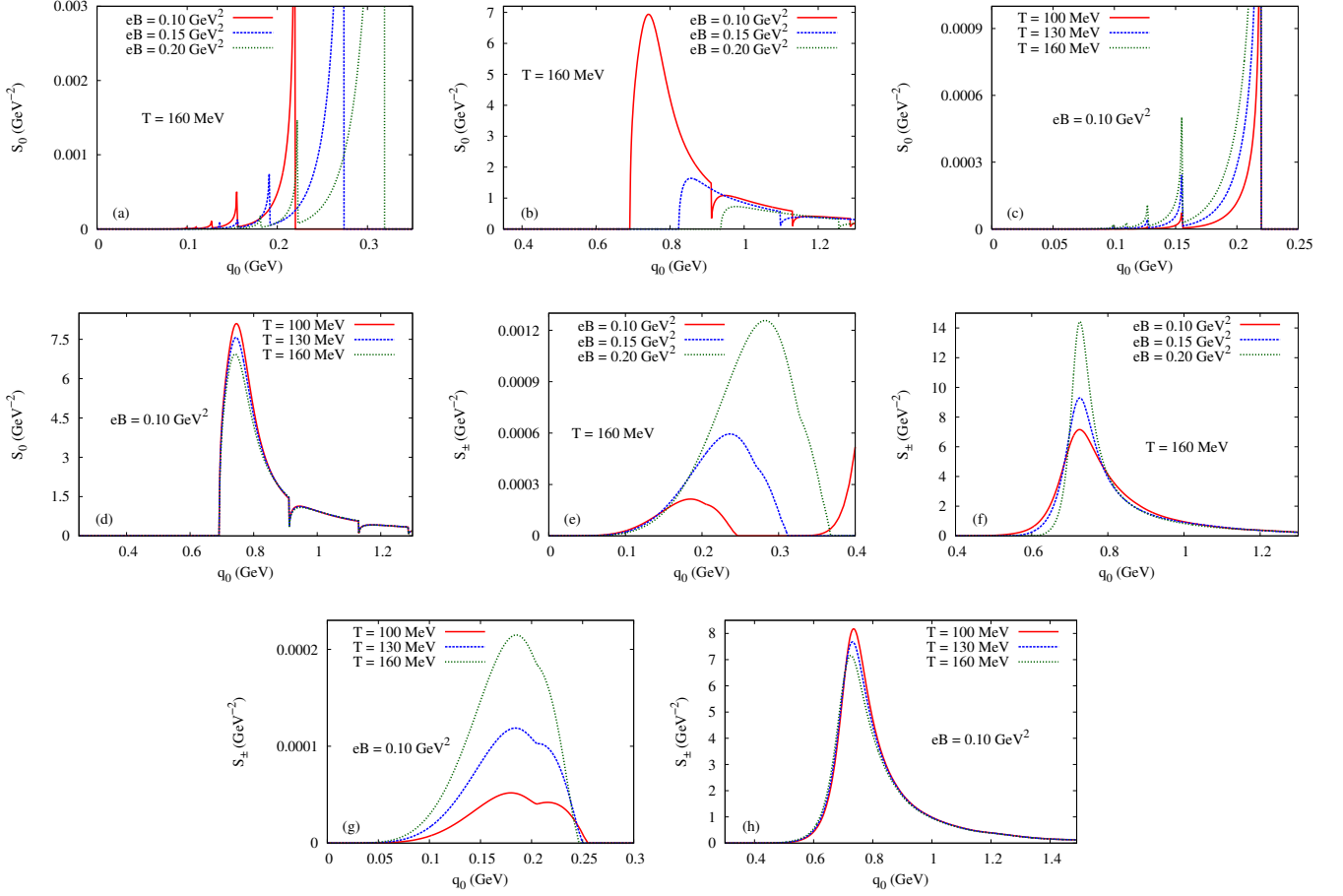


FIG. 7: The in-medium spectral functions of the ρ^0 at constant temperature (160 MeV) and at different values of the magnetic field (0.10, 0.15 and 0.20 GeV^2 respectively) (a) for q^0 from 0 to 0.35 GeV (b) for q^0 from 0.35 to 1.3 GeV. The same at constant magnetic field (0.10 GeV^2) and at different values of the temperature (100, 130 and 160 MeV respectively) (c) for q^0 from 0 to 0.25 GeV (d) for q^0 from 0.25 to 1.3 GeV. The in-medium spectral functions of the ρ^\pm at constant temperature (160 MeV) and at different values of the magnetic field (0.10, 0.15 and 0.20 GeV^2 respectively) (e) for q^0 from 0 to 0.41 GeV (f) for q^0 from 0.41 to 1.3 GeV. The same at constant magnetic field (0.10 GeV^2) and at different values of the temperature (100, 130 and 160 MeV respectively) (g) for q^0 from 0 to 0.30 GeV (h) for q^0 from 0.30 to 1.3 GeV.

Next in Fig. 6(a)-(d), the real part of the in-medium self energy functions of ρ at non-zero external magnetic field are presented. In Fig. 6(a), results of the ρ^0 at constant temperature (160 MeV) with four different values of the magnetic field (0.05, 0.10, 0.15 and 0.20 GeV^2 respectively) are shown. These plots are dominated by the “ B ” terms in Eq. (15). Small oscillatory behaviours in the plots arise due to the numerical principal value integrations. In Fig. 6(b), results are shown at a constant magnetic field (0.01 GeV^2) for three different values of the temperature (100, 130 and 160 MeV respectively). Effects of the increase in temperature though small, they make the real part larger. Analogous plots for ρ^\pm are presented in Fig. 6(c) and (d). Fig. 6(e) shows the comparison of the real part of the self energy function between ρ^0 and ρ^\pm . Results at two combinations of eB and T are given ($eB=0.10 \text{ GeV}^2$, $T=100 \text{ MeV}$ and $eB=0.20 \text{ GeV}^2$, $T=160 \text{ MeV}$ respectively). In both the cases, the real part of the ρ^0 self energy has a larger magnitude than that of ρ^\pm . This may be due to the fact that, the ρ^0 contains two charged particle in the loop whereas the ρ^\pm has only one. Having obtained the real and imaginary parts we present the in-medium spectral functions of ρ which contains both the real and imaginary parts of the self energy function. The spectral function is the imaginary part of the complete propagator and defined as,

$$S_{0,\pm}(q, eB, T) = \frac{\text{Im } \Pi_{0,\pm}}{(q^2 - m_\rho^2 + \text{Re } \Pi_{0,\pm})^2 + (\text{Im } \Pi_{0,\pm})^2} \quad (26)$$

In Fig. 7(a)-(d), spectral functions of ρ^0 are shown. In Fig. 7(a) and (b), results are shown at constant temperature

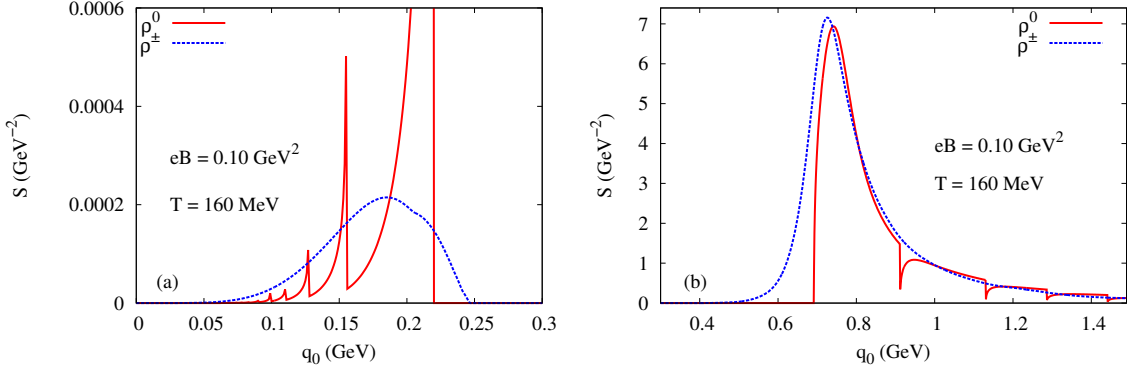


FIG. 8: The comparison of in-medium spectral functions between ρ^0 and ρ^\pm at $eB = 0.10 \text{ GeV}^2$ and $T = 160 \text{ MeV}$ (a) for q^0 from 0 to 0.30 GeV (a) for q^0 from 0.30 to 1.3 GeV.

(160 MeV) and at three different values of the magnetic field (0.10, 0.15 and 0.20 GeV^2 respectively). The spectral functions have the same threshold as the imaginary parts of the self energy, as is evident from Eq. (26). The spectral functions are shown in two parts, Fig. 7(a) shows the lower q^0 region dominated by the Landau terms whereas Fig. 7(b) shows the higher q^0 region, dominated by Unitary terms. It is seen from Fig. 7(a) that, with the increase of the magnetic field, the threshold of the spectral function shifts towards higher q^0 . However in Fig. 7(b) because of this shift, the spectral function misses the ρ mass pole, loses its Breit-Wigner shape, and becomes a continuum at large q^0 . This physically implies the “melting” of the ρ^0 at higher values of the magnetic field. In Fig. 7(c) and (d), the spectral functions at constant eB (0.10 GeV^2) for three different values of the temperature (100, 130 and 160 MeV respectively) are shown. The increase in temperature, increases the magnitude of the spectral function at low q^0 region, and decreases the magnitude at higher q^0 region without changing the threshold and shape.

In Fig. 7(e)-(h), similar plots of in-medium spectral function of ρ^\pm are presented. In Fig. 7(f), it is observed that with the increase in eB , the threshold of the spectral function seems to have a displacement towards higher q^0 . This is due the displacement of the Unitary cut contributions to the imaginary part of ρ^\pm self energy towards higher q^0 with the increase in eB , as can be seen from Fig. 5(g). However the Landau cut contribution is non-zero at every value of q^0 . So even if the Unitary cut threshold crosses the ρ pole at a high eB , the non-zero Landau cut contribution will maintain the Breit-Wigner shape of the spectral function. As the Landau cut contribution has a smaller magnitude, the spectral function will become narrow, which results in squeezing of ρ^\pm width and thus making it more stable. The effect of increase of temperature is similar to that of ρ^0 and is shown in Fig. 7(g) and (h). In Fig. 8, comparison of the ρ^0 and ρ^\pm spectral functions are shown, Fig. 8(a) shows the lower q^0 region and Fig. 8(b) shows the higher q^0 region.

Now we turn our attention to the evaluation of mass and dispersion relations. We first consider a vanishing transverse momentum for neutral as well as charged ρ mesons, i.e. $q^\mu \equiv (\omega, 0, 0, q_z)$ in Fig. 9 - 11. Although the transverse momenta of ρ^\pm is quantized as $q_\perp^2 = -(2n + 1)eB$ with $n = 0, 1, 2, \dots$, we will first neglect this trivial Landau shift in order to show the importance of the loop corrections of ρ^\pm . From the pole of the complete ρ propagator, the following dispersion relation is obtained for $q_\perp = 0$:

$$\det \left[\left(-q_\parallel^2 + m_\rho^2 \right) g^{\mu\nu} + q_\parallel^\mu q_\parallel^\nu - \text{Re} \bar{\Pi}_{0,\pm}^{\mu\nu} (q_\parallel, q_\perp = 0) \right] = 0. \quad (27)$$

The effective mass (m^*) of ρ is calculated by putting its three-momentum $\vec{q} = \vec{0}$ in the dispersion relation. Clearly, Eq. (27) will admit four solutions and we should get four modes of the effective mass and dispersion relation. Out of these modes, one is found to be unphysical and we are left with three physical modes of the effective mass and dispersion relation. These three modes corresponds to the three polarizations of the rho meson which is a spin-1 particle. In order to relate these modes with the physical spin state propagations, one needs to decompose the self energy tensor as well as the complete propagator in spin projection basis. In our approach, in order to avoid the complicated Lorentz structure of the self energy function at finite temperature and external magnetic field, we solve Eq. (27) instead. Thus in our case, although we have three modes, the correspondence with definite spin states is not obvious. Since, we have taken $\vec{q} = (0, 0, q_z)$, two modes are identical and we are left with two distinct modes. We refer to these modes as Mode-I and Mode-II respectively.

In Fig. 9(a)-(d), the effective mass (m_0^*) of ρ^0 is shown. In the Fig. 9(a) and (b), m_0^* is plotted as a function of eB at three different temperatures (100, 130 and 160 MeV) for Mode-I and Mode-II respectively. We find significant

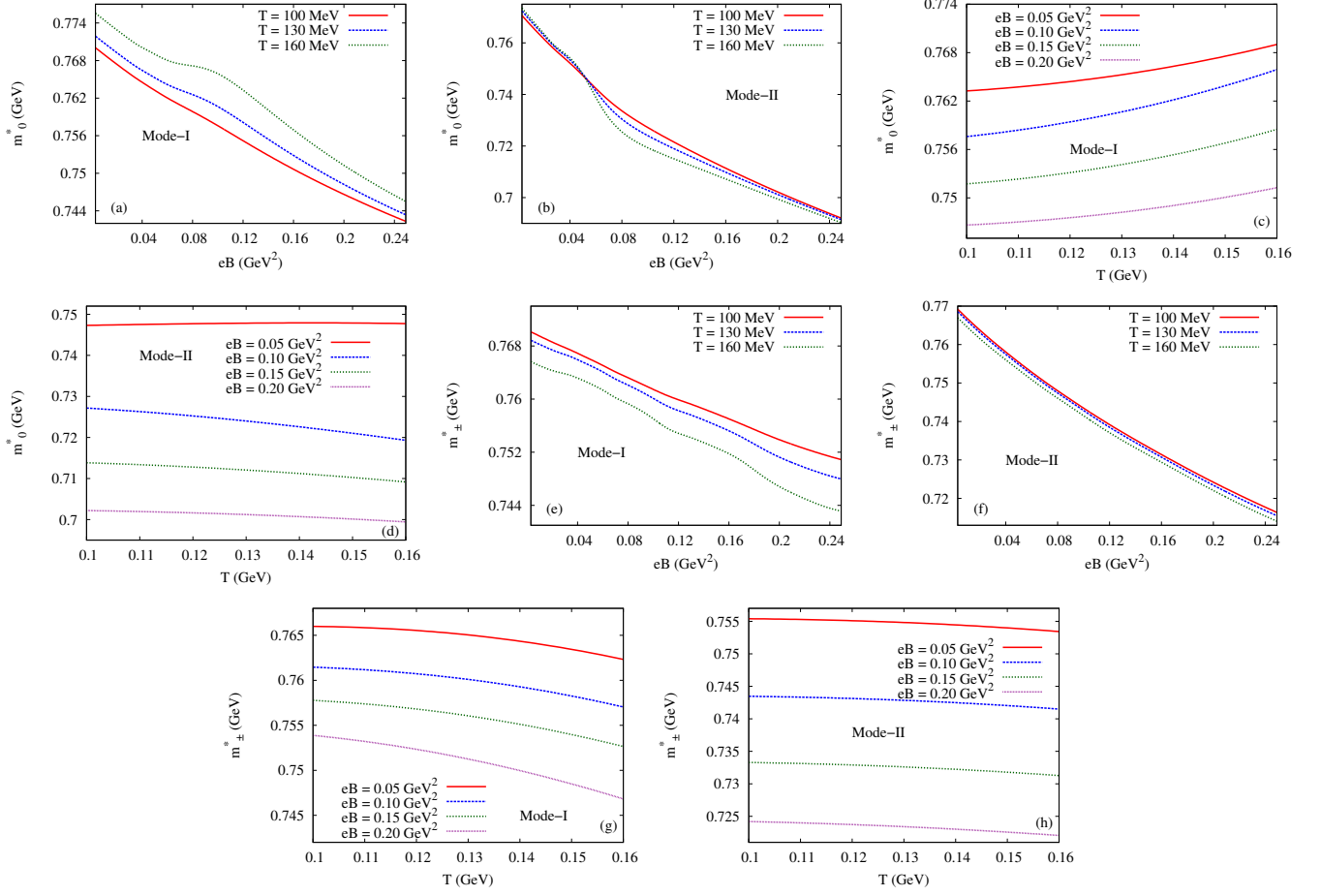


FIG. 9: The effective masses of the ρ^0 vs eB at different values of temperatures (100, 130 and 160 MeV) for (a) Mode-I and (b) Mode-II. The effective masses of the ρ^0 vs T at different values of the magnetic field (0.05, 0.10, 0.15 and 0.20 GeV²) for (c) Mode-I and (d) Mode-II. The effective masses of the ρ^{\pm} vs eB at different values of temperatures (100, 130 and 160 MeV) for (a) Mode-I and (b) Mode-II. The effective masses of the ρ^{\pm} vs T at different values of the magnetic field (0.05, 0.10, 0.15 and 0.20 GeV²) for (c) Mode-I and (d) Mode-II.

decrease of ρ^0 mass with the increase of eB in both modes which is due to a strong positive contribution coming from the real part of the self energy. This decrease of m_0^* is more in Mode-I as compared to Mode-II. In Fig. 9(c)-(d), m_0^* is plotted as a function of the T at four different values of eB (0.05, 0.10, 0.15 and 0.20 GeV²) for Mode-I and Mode-II. The variation of m_0^* is slow as the contribution of the “ BT ” terms are small compared to the “ B ” terms as seen from Eqs. (15) and (16). We find small increase (decrease) of m_0^* with the increase of T in Mode-I (Mode-II).

In Fig. 9(e)-(h), corresponding plots are shown for ρ^{\pm} . The effective mass (m_{\pm}^*) of ρ^{\pm} shows similar behaviour as the ρ^0 . Due to the presence of one Laguerre polynomial in the expression of the real part of thermal self energy in Eq. (20), small oscillatory behaviour is present in the Fig. 9(a). In the lower panel, the m_{\pm}^* is decreasing with the increase in temperature in both the modes.

Having obtained the effective masses, we now proceed to present the dispersion relations of rho meson. In Fig. 10(a)-(d), dispersion curves of ρ^0 are shown. We have plotted the energy (ω_0) of ρ^0 as a function of q_z taking $q_x = q_y = 0$. In Fig. 10(a) and (b), dispersion curves are shown at constant temperature (160 MeV) and at four different values of eB (0.05, 0.10, 0.15 and 0.20 GeV²) for Mode-I and Mode-II respectively. In all the cases, the dispersion curves are well separated at $q_z = 0$ (which is actually the effective mass). As the momentum increases, the kinetic energy term dominates over the self energy corrections and the dispersion relation becomes light-like. In Fig. 10(c) and (d), dispersion curves are shown at constant eB (0.10 GeV²) and at three different values of the temperature (100, 130 and 160 MeV) for Mode-I and Mode-II. The separation among the curves are very small due to smallness of the “ BT ” terms as compared to “ B ” terms in the real part of self energy. In Fig. 10(e)-(h), corresponding plots are shown for ρ^{\pm} . In this case we find results similar to the ρ^0 except the fact that the separation among the dispersion curves

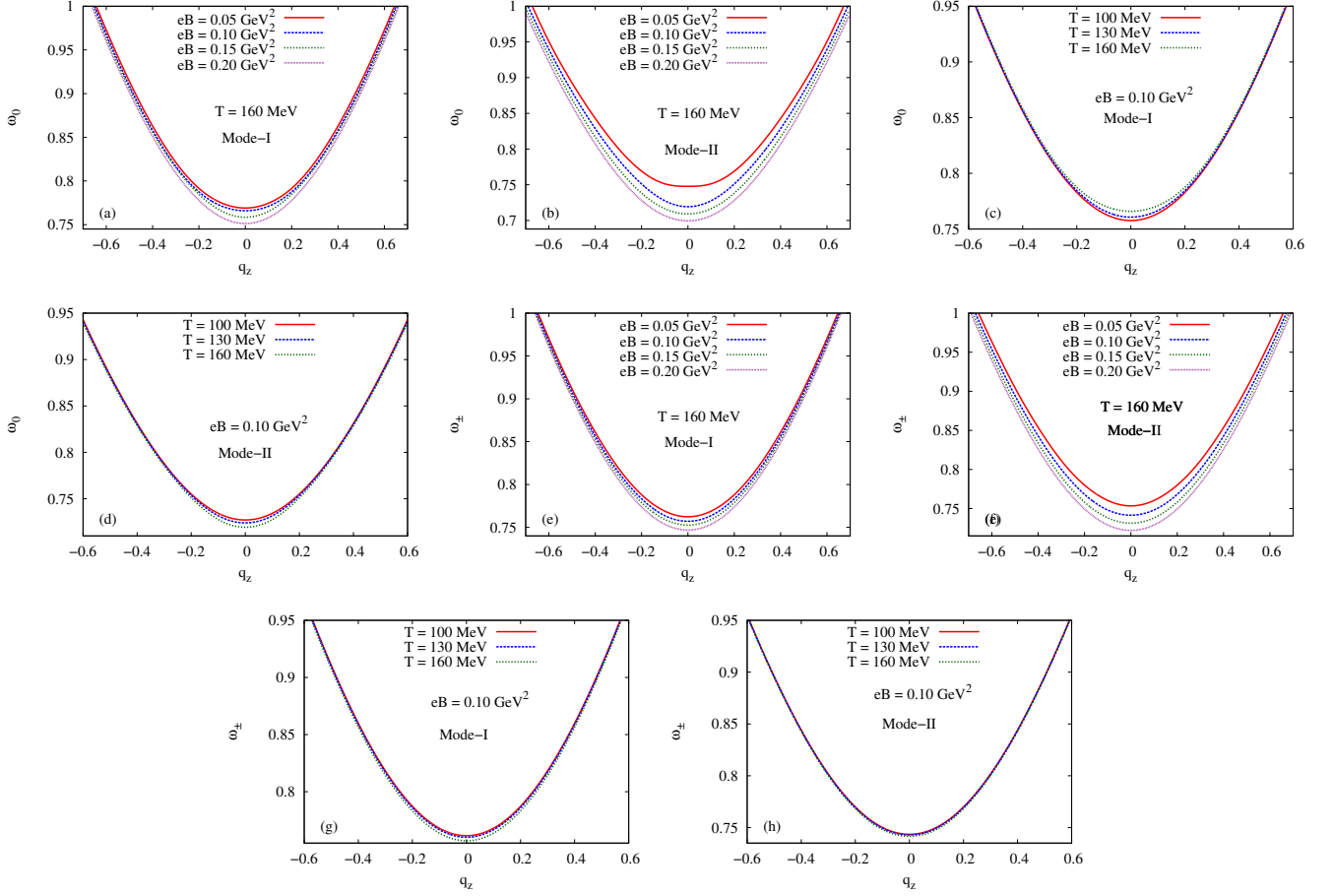


FIG. 10: The dispersion curves of the ρ^0 at constant temperature (160 MeV) and at different values of the magnetic field (0.05, 0.10, 0.15 and 0.20 GeV^2 respectively) for (a) Mode-I and (b) Mode-II. The same at constant magnetic field (0.10 GeV^2) and at different values of the temperature (100, 130, and 160 MeV respectively) for (a) Mode-I and (b) Mode-II. The dispersion curves of the ρ^\pm at constant temperature (160 MeV) and at different values of the magnetic field (0.05, 0.10, 0.15 and 0.20 GeV^2 respectively) for (a) Mode-I and (b) Mode-II. The same at constant magnetic field (0.10 GeV^2) and at different values of the temperature (100, 130, and 160 MeV respectively) for (a) Mode-I and (b) Mode-II.

becomes less. This is due to the fact that the real part of the ρ^\pm self energy has a lower magnitude than that of ρ^0 .

In Fig. 11, we have shown comparison of effective masses and dispersion curves between ρ^0 and ρ^\pm at constant temperature (160 MeV). From Fig. 11(a), it is observed that, when $eB \approx 0$ both the ρ^0 and ρ^\pm have identical effective masses. This is because of the fact that the ρ^0 and ρ^\pm self energies at $eB=0$ are equal. With the increase in eB , the splitting between them increases. Moreover the effect of the external magnetic field is more on ρ^0 than that on ρ^\pm . Fig. 11(b) shows comparison plots of dispersion curves at constant magnetic field (0.10 GeV^2).

Now we will introduce non-zero three momenta for the charged rho mesons. Keeping in mind the Landau quantization of the transverse momenta of ρ^\pm , we parametrize the ρ^\pm four momenta as,

$$q^\mu \equiv \left(q^0, \sqrt{(2n+1)eB} \cos \phi, \sqrt{(2n+1)eB} \sin \phi, 0 \right) \quad ; \quad n = 0, 1, 2, 3, \dots, \quad (28)$$

where ϕ is the azimuthal angle. In Fig. (12), we have shown the ρ^\pm spectral function as a function of the invariant mass ($\sqrt{q^2} = \sqrt{q_0^2 - \vec{q}^2}$) of rho meson. Results are shown at a constant magnetic field (0.10 GeV^2), temperature (160 MeV) and azimuthal angle ($\frac{\pi}{4}$) with four values of n (0, 1, 2 and 3). The peak of the spectral function increases with increase of n with very small shifts towards higher $\sqrt{q^2}$ making the ρ^\pm more stable at higher transverse momenta. We have not shown the azimuthal angle (ϕ) dependence of the spectral function since it is insignificantly small. The dispersion relation for ρ^\pm will follow from the pole of the complete propagator. For simplicity we have taken the

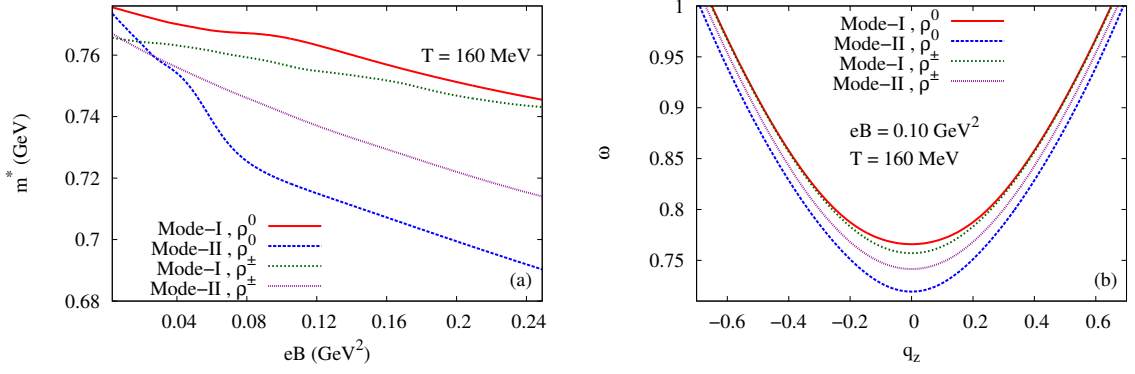


FIG. 11: The comparison of (a) effective mass (b) dispersion curve between the ρ^0 and ρ^\pm at constant temperature (160 MeV) and magnetic field (0.1 GeV^2) for Mode-I and Mode-II.

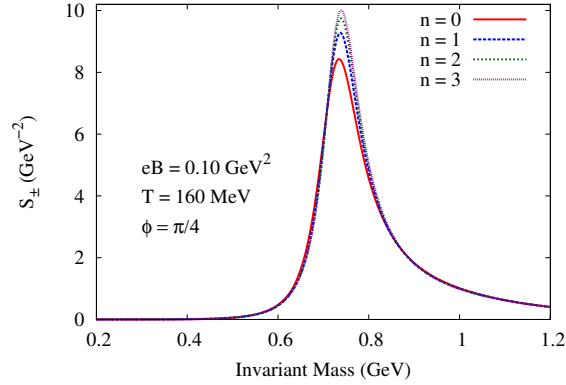


FIG. 12: The in-medium spectral functions of the ρ^\pm at constant temperature (160 MeV), magnetic field (0.10 GeV^2) and azimuthal angle ($\frac{\pi}{4}$) at four Landau levels ($n = 0, 1, 2$ and 3)

azimuthal angle $\phi = (\pi/2)$, for which $\vec{q} \equiv (0, \sqrt{(2n+1)eB}, 0)$ and the corresponding dispersion relation is,

$$\det \left[(-q_0^2 + (2n+1)eB + m_\rho^2) g^{\mu\nu} + q^\mu q^\nu - \text{Re } \bar{\Pi}_{0,\pm}^{\mu\nu} \left(q^0, q_x = 0, q_y = \sqrt{(2n+1)eB}, q_z = 0 \right) \right] = 0. \quad (29)$$

Clearly, the effective mass obtained from Eq. (29) will be function of the Landau level n in addition to temperature (T) and magnetic field (eB). As before, we have obtained two distinct physical modes for the n -dependent effective mass ($m_\pm^*(n)$) of ρ^\pm . We will refer these modes as Mode-I and Mode-II respectively. In Fig. 13, $m_\pm^*(n)$ is plotted as a function of eB , T and n in the left, middle and right panels respectively at azimuthal angle ($\phi = \pi/2$). Fig. 13(a) shows $m_\pm^*(n)$ for Mode-I at constant temperature (160 MeV) and at four values of n . It is clear that the trivial Landau term completely dominates over the self-energy correction and effective mass monotonically increases with the increase of eB . Fig. 13(b) shows corresponding plot for Mode-II. In Fig. 13(c), $m_\pm^*(n)$ for Mode-I is shown as a function of the temperature at six different combinations of eB and n . Since the variation of T affects only the self energy part which is subleading compared to the dominant trivial Landau term, we see no significant variation of effective mass with temperature. Corresponding plot for Mode-II is shown in Fig. 13(d). Finally, we have shown $m_\pm^*(n)$ vs n at constant temperature (160 MeV) and at four different values of the magnetic field ($0.05, 0.10, 0.15$ and 0.20 GeV^2) for Mode-I and Mode-II in Fig. 13(e) and Fig. 13(f) respectively. Here also the self energy correction have insignificant effect with respect to the Landau level term ($(2n+1)eB$) so that the separation among them increases with the increase of n .

Until now, we have neglected the trivial coupling between the magnetic moment of ρ^\pm and the external magnetic field. Following Ref. [8], the dispersion relation of ρ^\pm (without loop correction) under external magnetic field is given

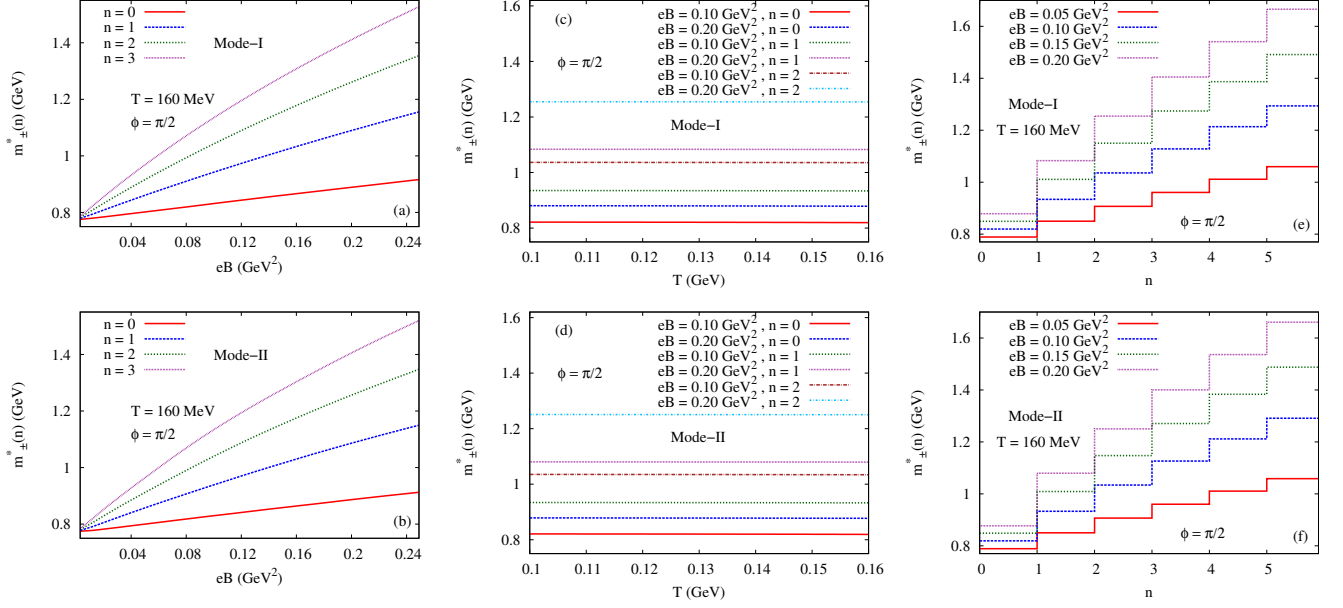


FIG. 13: The Landau level (n) dependent effective mass of ρ^\pm at $\phi = \pi/2$ (left panel) as a function of eB at constant temperature (160 MeV) and at four values of n (middle panel) as a function of T at different combinations of eB and n (right panel) as a function of n at constant temperature (160 MeV) and four different values of eB . The upper and lower panel shows results for Mode-I and Mode-II respectively.

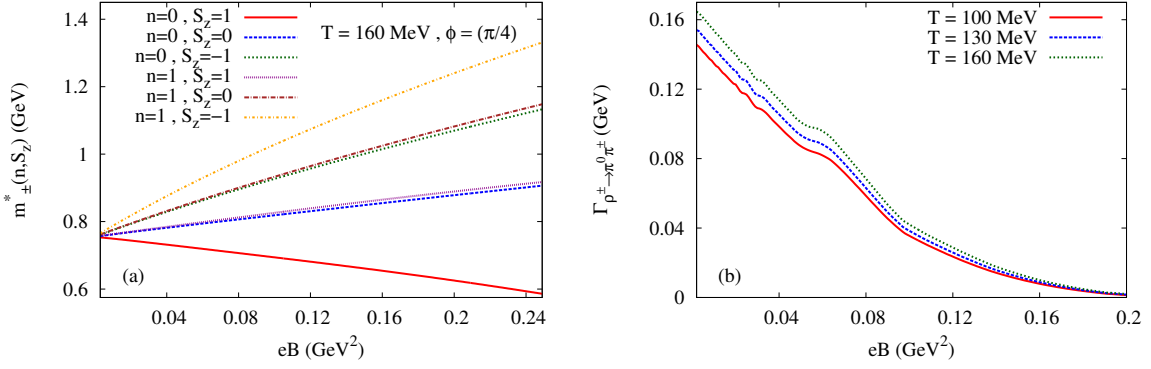


FIG. 14: (a) The effective mass of charged rho as a function of eB at $T = 160$ MeV, $\phi = \pi/4$ and at different combinations of n and S_z . (b) The decay width of charged rho as a function of eB at different temperatures.

by,

$$q_0^2 = q_z^2 + (2n + 1 - 2S_z)eB + m_\rho^2, \quad (30)$$

where, $S_z \in (1, 0, -1)$ and $n \geq 0$ are the spin projections on the field axis and Landau level index respectively. It is evident from the above equation, that the effective mass of ρ^\pm will be dominated by the leading order trivial contribution coming from the second term on the R.H.S. which is a linear term in eB . Corresponding order corrections in the effective mass due to the self-energy contribution are subleading compared to this trivial term and this can be noticed in Fig. 9(g)-(h) and Fig. 13(c)-(d). In view of this, let us approximate the contribution of self energy in different modes (which corresponds to different spin projections) by the spin-averaged one. So the dispersion relation of ρ^\pm becomes,

$$q_0^2 = q_z^2 + (2n + 1 - 2S_z)eB + m_\rho^2 - \text{Re} \Pi_\pm \left(q^0, q_x = \sqrt{(2n + 1)eB} \cos \phi, q_y = \sqrt{(2n + 1)eB} \sin \phi, q_z \right), \quad (31)$$

where, Π_{\pm} is defined in Eq. (25). The effective mass $m_{\pm}^*(n, S_z)$ obtained from the above equation by putting $q_z = 0$, will depend on n and S_z in addition to eB , T and ϕ . In Fig. 14(a), we have plotted $m_{\pm}^*(n, S_z)$ as a function of eB at $T = 160$ MeV and $\phi = (\pi/4)$ for the two Landau levels with different spin projections. The only case where the effective mass decreases rapidly with the increase of eB is for $n = 0$ and $S_z = 1$ as evident from the R.H.S. of Eq. (31). This is due to the fact that, with the increase of eB , both the terms $(2n + 1 - 2S_z)eB$ as well as $-\text{Re } \Pi_{\pm}$ gives strong negative contributions. For the other combinations of n and S_z , there is a competition between the trivial term and the self energy; the term $(2n + 1 - 2S_z)eB$ gives strong positive contribution, whereas the term $-\text{Re } \Pi_{\pm}$ always gives small negative contribution which is subleading as compared to the trivial term. This leads to the fact that $m^*(n, S_z)$ increases monotonically with eB except the case when $n = 0$ and $S_z = 1$. Moreover, the graphs for $n = 0, S_z = 0$ and $n = 1, S_z = 1$ (both having equal trivial contributions) lie almost on top of each other. The same behaviour is seen in the graphs for $n = 0, S_z = -1$ and $n = 1, S_z = 0$ as well. It is to be noted that, the real part of the self energy in Eq. (31) consists of two parts, the ‘‘B’’ part and the ‘‘BT’’ part. The T and ϕ dependent part (‘‘BT’’) is very small as compared to the magnetic field dependent vacuum part (‘‘B’’). For this reason, the effect of T and ϕ on $m^*(n, S_z)$ will be negligibly small and thus we have not shown its variation with T and ϕ .

We conclude this section with the result on the decay width of charged rho meson in presence of the magnetic field. We define the decay width of ρ^{\pm} in its lowest energy state as,

$$\Gamma_{\rho^{\pm} \rightarrow \pi^0 \pi^{\pm}}(eB, T) = \frac{1}{m_{\pm}^*(0, 1)} \int_0^{2\pi} \frac{d\phi}{2\pi} \text{Im } \Pi_{\pm} \left(q^0 = m_{\pm}^*(0, 1), q_x = \sqrt{eB} \cos \phi, q_y = \sqrt{eB} \sin \phi, q_z = 0 \right), \quad (32)$$

where we have made an average over the azimuthal angle ϕ . The decay width is shown in Fig. 14(b) as a function of eB at three different values of temperature (100, 130 and 160 MeV respectively). With the increase in eB , the decay width decreases and this can be understood from Fig. 5(g) where the magnitude of the Unitary cut contribution to the self energy decreases with the increase in eB around the rho mass pole. The oscillatory behaviour in the decay width is due to the oscillatory behaviour of the Landau cut contribution of the self energy as can be seen from Fig. 5(c). At very high value of eB , the value of the decay width becomes close to zero and the ρ^{\pm} becomes stable against decay into two pions. The decay width increases with the increase in temperature and can be understood from Fig. 5(d) and (h) where the imaginary part increases with the increase in temperature. This physically means that ρ^{\pm} is more unstable at a higher temperature and at lower eB .

VII. SUMMARY AND DISCUSSIONS

We have made comprehensive study of the self energies of ρ meson using effective $\rho\pi\pi$ interaction at finite temperature and arbitrary external magnetic field including all the Landau levels in the propagators of the loop particle in our calculations. We have also explicitly worked out the analytic structure of the self energy at finite temperature and arbitrary non-zero external magnetic field. The kinematic domains of the imaginary part of the self energy in the complex q^0 plane are found to be different for ρ^0 and ρ^{\pm} as well as from the $eB = 0$ case. For vanishing three momentum of the ρ , we have observed Landau cut contributions to the imaginary part of the self energy at non-zero magnetic field which is absent at zero magnetic field. While calculating the real part of the self energy, we have taken the magnetic field dependent vacuum contributions which is usually ignored in most of the works in the literature and this term produces dominating contribution to the effective mass and dispersion relations. The in-medium spectral functions obtained from the spin-averaged self energy is found to be quite different for ρ^0 and ρ^{\pm} . The ‘‘Threshold Singularities’’ in the ρ^0 spectral function give rise to spike like structures which is absent in case of ρ^{\pm} . It is also shown quantitatively that, the ρ^0 meson ‘‘melts’’ at high magnetic field whereas ρ^{\pm} does not. From the pole of the complete ρ propagator, we have evaluated its effective mass and dispersion relations. First we have presented results neglecting the trivial Landau shift to the ρ^{\pm} transverse momenta in order to see the effect of self energy correction which is a function of both T and eB . This kind of situation may occur in principle when different species of charged particle are present in the system all of which undergoing trivial Landau shifts. In that case, the real part of the self energy will play the deciding role in the characterization of effective masses. We find two distinct physical modes for the effective mass and dispersion relation. The effective mass of ρ is seen to decrease with the increase in magnetic field. We have also taken the trivial coupling between the magnetic moment of charged rho with the external magnetic field along with the trivial Landau shifts. Incorporation of this term has made the effective mass of ρ^{\pm} to be dependent on the spin projection along with the Landau level n . For a particular combination, $n = 0$ and $S_z = 1$, the effective mass decreases very rapidly with the increase in eB and charged rho condensation may occur. The decay width of ρ^{\pm} is found to be decreasing with the increase in eB and at certain higher value of eB , the ρ^{\pm} becomes stable against decay into pions.

Acknowledgement

Snigdha Ghosh acknowledges Center for Nuclear Theory, Variable Energy Cyclotron Centre and Department of Atomic Energy, Government of India for support.

Appendix A: Calculation of $\text{Re}(\Pi_0^{\mu\nu})_B$

In this appendix we shall briefly sketch how to obtain Eq. (17). We have

$$\begin{aligned} (\Pi_0^{\mu\nu})_B &= i \int \frac{d^4 k}{(2\pi)^4} \mathcal{N}^{\mu\nu} \Delta_B(k) \Delta_B(p = q - k) \\ &= i \int \frac{d^4 k}{(2\pi)^4} \mathcal{N}^{\mu\nu} \sum_{l=0}^{\infty} \sum_{n=0}^{\infty} \left[\frac{\phi_l(\alpha_k) \phi_n(\alpha_k)}{(k_{\parallel}^2 - m_l^2 + i\epsilon)(p_{\parallel}^2 - m_n^2 + i\epsilon)} \right]. \end{aligned}$$

Using standard Feynman parametrization, we combine the denominators of the two propagators and obtain

$$(\Pi_0^{\mu\nu})_B = i \sum_{l=0}^{\infty} \sum_{n=0}^{\infty} \int_0^1 dx \int \frac{d^2 k_{\perp}}{(2\pi)^2} \phi_l(\alpha_k) \phi_n(\alpha_k) \int \frac{d^2 k_{\parallel}}{(2\pi)^2} \frac{\mathcal{N}^{\mu\nu}}{[(k_{\parallel} - xq_{\parallel})^2 - \Delta_{n,l}]^2},$$

where, $\Delta_{n,l} = \Delta + eB(2l + 1 - 2xl + 2xn)$. Shifting momenta $k_{\parallel} \rightarrow (k_{\parallel} + xq_{\parallel})$ and performing the k_{\parallel} integration using dimensional regularization we get,

$$\begin{aligned} (\Pi_0^{\mu\nu})_B &= \left(\frac{g_{\rho\pi\pi}^2 q_{\parallel}^2}{4\pi} \right) i \sum_{l=0}^{\infty} \sum_{n=0}^{\infty} \int_0^1 dx \int \frac{d^2 k_{\perp}}{(2\pi)^2} \phi_l(\alpha_k) \phi_n(\alpha_k) \left[\left(q_{\parallel}^2 g_{\parallel}^{\mu\nu} - q_{\parallel}^{\mu} q_{\parallel}^{\nu} \right) \frac{1}{2} \Gamma \left(1 - \frac{d}{2} \right) \left(\frac{1}{\Delta_{n,l}} \right)^{1-d/2} \right. \\ &\quad \left. - q_{\parallel}^2 k_{\perp}^{\mu} k_{\perp}^{\nu} \Gamma \left(2 - \frac{d}{2} \right) \left(\frac{1}{\Delta_{n,l}} \right)^{2-d/2} \right]_{d \rightarrow 2}. \end{aligned}$$

Now using the $\overline{\text{MS}}$ scheme we subtract out the divergence arising from the pole of the Gamma function. The remaining k_{\perp} integration is convergent and can be evaluated using the orthogonality properties of the Laguerre polynomials present in the numerator which also remove one sum from the double sum. Then the $(\Pi_0^{\mu\nu})_B$ can be written in the following compact form

$$(\Pi_0^{\mu\nu})_B = \left(\frac{g_{\rho\pi\pi}^2 q_{\parallel}^2}{32\pi^2} \right) \int_0^1 dx \left[\left(q_{\parallel}^2 g_{\parallel}^{\mu\nu} - q_{\parallel}^{\mu} q_{\parallel}^{\nu} \right) S_{\parallel} + q_{\parallel}^2 g_{\perp}^{\mu\nu} S_{\perp} \right] \quad (\text{A1})$$

where, S_{\parallel} and S_{\perp} are given by,

$$S_{\parallel} = \sum_{n=0}^{\infty} \left[2eB \ln \left(\frac{\Delta_{n,n}}{\mu_0} \right) \right] \quad (\text{A2})$$

$$S_{\perp} = \sum_{n=0}^{\infty} eB \left[\frac{2n+1}{\Delta_{n,n}} + \frac{2n+2}{\Delta_{n+1,n}} \right]. \quad (\text{A3})$$

The infinite sums in Eq. (A2) and (A3) are divergent and can be regularized using derivative regularization technique [41]. To do this we differentiate them with respect to $M = q_{\parallel}^2$ twice and obtain convergent sums, which are expressible in terms of polygamma functions (Ψ , Ψ' and Ψ''),

$$\left(\frac{\partial^2 S_{\parallel}}{\partial M^2} \right) = \frac{-x^2(1-x)^2}{2eB} \Psi' \left(\frac{\Delta}{2eB} + \frac{1}{2} \right) \quad (\text{A4})$$

$$\begin{aligned} \left(\frac{\partial^2 S_{\perp}}{\partial M^2} \right) &= \frac{x^2(1-x)^2}{2(eB)^2} \left[\Psi' \left(\frac{\Delta}{2eB} + \frac{1}{2} \right) + \left(\frac{\Delta}{4eB} \right) \Psi'' \left(\frac{\Delta}{2eB} + \frac{1}{2} \right) + \right. \\ &\quad \left. \Psi' \left(\frac{\Delta}{2eB} + \frac{1}{2} + x \right) + \left(\frac{\Delta}{4eB} + \frac{2x-1}{4} \right) \Psi'' \left(\frac{\Delta}{2eB} + \frac{1}{2} + x \right) \right]. \end{aligned} \quad (\text{A5})$$

Integrating Eq. (A4) and (A5), and substituting S_{\parallel} and S_{\perp} into Eq. (A1), we obtain,

$$(\Pi_0^{\mu\nu})_B = \left(\frac{g_{\rho\pi\pi}^2 q_{\parallel}^2}{32\pi^2} \right) \int_0^1 dx \left[\left(q_{\parallel}^2 g_{\parallel}^{\mu\nu} - q_{\parallel}^{\mu} q_{\parallel}^{\nu} \right) \left\{ 2eB \ln \Gamma \left(\frac{\Delta}{2eB} + \frac{1}{2} \right) + C_1 q_{\parallel}^2 + C_2 \right\} \right. \\ \left. + q_{\parallel}^2 g_{\perp}^{\mu\nu} \left\{ \frac{\Delta}{2eB} \Psi \left(\frac{\Delta}{2eB} + \frac{1}{2} \right) + \left(\frac{\Delta}{2eB} - \frac{1}{2} + x \right) \Psi \left(\frac{\Delta}{2eB} + \frac{1}{2} + x \right) + C_3 q_{\parallel}^2 + C_4 \right\} \right] \quad (\text{A6})$$

where C_1, C_2, C_3 and C_4 are integration constants and independent of q_{\parallel}^2 but can be functions of x and eB . These constants have to be chosen such that in the limit of zero magnetic field, we get back the vacuum self energy as given in Eq. (3) i.e.

$$\lim_{eB \rightarrow 0} (\Pi_0^{\mu\nu})_B = (\Pi^{\mu\nu})_{vac}. \quad (\text{A7})$$

From Eq. (A7), we get $C_1 = C_3 = -x(1-x) \ln \left(\frac{2eB}{\mu_0} \right)$, $C_2 = m^2 \ln \left(\frac{2eB}{\mu_0} \right)$ and $C_4 = m^2 \ln \left(\frac{2eB}{\mu_0} \right) - m^2$. Substituting the values of C_1, C_2, C_3 and C_4 into Eq. (A6) and taking the real part, we get Eq. (17).

Appendix B: Calculation of $\text{Re}(\Pi_{\pm}^{\mu\nu})_B$

We have

$$(\Pi_{\pm}^{\mu\nu})_B = i \int \frac{d^4 k}{(2\pi)^4} \mathcal{N}^{\mu\nu} \Delta_0(k) \Delta_B(p = q - k) \\ = i \int \frac{d^4 k}{(2\pi)^4} \mathcal{N}^{\mu\nu} \sum_{n=0}^{\infty} \left[\frac{\phi_n(\alpha_p)}{(k^2 - m_{\pi}^2 + i\epsilon)(p_{\parallel}^2 - m_n^2 + i\epsilon)} \right].$$

Using standard Feynman parametrization, we combine the denominators of the two propagators and obtain

$$(\Pi_{\pm}^{\mu\nu})_B = i \sum_{n=0}^{\infty} \int_0^1 dx \int \frac{d^2 k_{\perp}}{(2\pi)^2} \phi_n(\alpha_p) \int \frac{d^2 k_{\parallel}}{(2\pi)^2} \frac{\mathcal{N}^{\mu\nu}}{[(k_{\parallel} - xq_{\parallel})^2 - \Delta_n]^2},$$

where, $\Delta_n = \Delta + x(2n+1)eB - (1-x)k_{\perp}^2$. Shifting momenta $k_{\parallel} \rightarrow (k_{\parallel} + xq_{\parallel})$ and performing the k_{\parallel} integration using dimensional regularization we get,

$$(\Pi_{\pm}^{\mu\nu})_B = \left(\frac{g_{\rho\pi\pi}^2}{4\pi} \right) \sum_{n=0}^{\infty} \int_0^1 dx \int \frac{d^2 k_{\perp}}{(2\pi)^2} \phi_n(\alpha_p) \left[A^{\mu\nu} \Gamma \left(1 - \frac{d}{2} \right) \left(\frac{1}{\Delta_n} \right)^{1-d/2} - B^{\mu\nu} \Gamma \left(2 - \frac{d}{2} \right) \left(\frac{1}{\Delta_n} \right)^{2-d/2} \right]_{d \rightarrow 2},$$

where $A^{\mu\nu}$ and $B^{\mu\nu}$ are given by,

$$A^{\mu\nu} = \frac{1}{2} \left[q^4 g_{\parallel}^{\mu\nu} + q_{\parallel}^2 q^{\mu} q^{\nu} - q^2 (q^{\mu} q_{\parallel}^{\nu} + q^{\nu} q_{\parallel}^{\mu}) \right] \quad (\text{B1}) \\ B^{\mu\nu} = q^4 \left(x^2 q_{\parallel}^{\mu} q_{\parallel}^{\nu} + k_{\perp}^{\mu} k_{\perp}^{\nu} + x q_{\parallel}^{\mu} k_{\perp}^{\nu} + x q_{\parallel}^{\nu} k_{\perp}^{\mu} \right) + (x q_{\parallel}^2 + q_{\perp} \cdot k_{\perp})^2 q^{\mu} q^{\nu} \\ - q^2 (x q_{\parallel}^2 + q_{\perp} \cdot k_{\perp}) (x q^{\mu} q_{\parallel}^{\nu} + x q^{\nu} q_{\parallel}^{\mu} + q^{\mu} k_{\perp}^{\nu} + q^{\nu} k_{\perp}^{\mu}).$$

Now as before we subtract out the divergences arising from the pole of the Gamma function and obtain,

$$(\Pi_{\pm}^{\mu\nu})_B = \left(\frac{-g_{\rho\pi\pi}^2}{4\pi} \right) \int_0^1 dx \int \frac{d^2 k_{\perp}}{(2\pi)^2} \left[A^{\mu\nu} \tilde{S}_{\parallel} + B^{\mu\nu} \tilde{S}_{\perp} \right] \quad (\text{B2})$$

where, \tilde{S}_{\parallel} and \tilde{S}_{\perp} are given by,

$$\tilde{S}_{\parallel} = \sum_{n=0}^{\infty} \left[\phi_n(\alpha_p) \ln \left(\frac{\Delta_n}{\mu_0} \right) \right] \quad (\text{B3})$$

$$\tilde{S}_{\perp} = \sum_{n=0}^{\infty} \left[\frac{\phi_n(\alpha_p)}{\Delta_n} \right]. \quad (\text{B4})$$

Differentiating Eq. (B3) with respect to q_{\parallel}^2 , we get,

$$\frac{\partial \tilde{S}_{\parallel}}{\partial q_{\parallel}^2} = \sum_{n=0}^{\infty} \left[-x(1-x) \frac{\phi_n(\alpha_p)}{\Delta_n} \right]. \quad (\text{B5})$$

To evaluate the infinite sums in Eq. (B4) and (B5), we introduce a new parameter z and write

$$\frac{1}{\Delta_n} = \int_0^1 \frac{dz}{m_{\pi}^2} z^{\Delta_n/m_{\pi}^2 - 1}. \quad (\text{B6})$$

Substituting Eq. (B6) into Eq. (B4) and (B5) and using the identity $\sum_{n=0}^{\infty} L_n(t) z^n = (1-z)^{-1} \exp\left(\frac{tz}{z-1}\right)$ for $|z| \leq 1$, we obtain,

$$\tilde{S}_{\parallel} = \int_0^1 \frac{dz}{\ln z} z^{\Delta/m_{\pi}^2 - 1} \text{sech}\left(x \frac{eB}{m_{\pi}^2} \ln z\right) e^{\zeta} + \tilde{C}_1 \quad (\text{B7})$$

$$\tilde{S}_{\perp} = \int_0^1 \frac{dz}{m_{\pi}^2} z^{\Delta/m_{\pi}^2 - 1} \text{sech}\left(x \frac{eB}{m_{\pi}^2} \ln z\right) e^{\zeta} \quad (\text{B8})$$

where, \tilde{C}_1 is the constant of the q_{\parallel}^2 -integration and is independent of q_{\parallel}^2 which is chosen to be zero and

$$\zeta = -(1-x) \frac{k_{\perp}^2}{m_{\pi}^2} \ln z + \alpha_p \tanh\left(x \frac{eB}{m_{\pi}^2} \ln z\right).$$

Substituting Eq. (B7) and (B8) into Eq. (B2) we get,

$$(\Pi_{\pm}^{\mu\nu})_B = \left(\frac{-g_{\rho\pi\pi}^2}{4\pi} \right) \int_0^1 \int_0^1 dx dz z^{\Delta/m_{\pi}^2 - 1} \text{sech}\left(x \frac{eB}{m_{\pi}^2} \ln z\right) \int \frac{d^2 k_{\perp}}{(2\pi)^2} e^{\zeta} \left[\frac{A^{\mu\nu}}{\ln z} + \frac{B^{\mu\nu}}{m_{\pi}^2} \right].$$

In order to perform the $d^2 k_{\perp}$ integration, we rewrite the ζ by completing the square in k_{\perp} as bellow,

$$\zeta = -\tilde{\zeta}(k_{\perp} - yq_{\perp})^2 - y(1-x) \frac{q_{\perp}^2}{m_{\pi}^2} \ln z$$

where $\tilde{\zeta} = (1-x) \frac{\ln z}{m_{\pi}^2} + \frac{1}{eB} \tanh\left(x \frac{eB}{m_{\pi}^2} \ln z\right)$ and $y = \frac{1}{\tilde{\zeta} eB} \tanh\left(x \frac{eB}{m_{\pi}^2} \ln z\right)$. Now shifting momenta $k_{\perp} \rightarrow (k_{\perp} + yq_{\perp})$ and performing the remaining Gaussian integration of the variable $|\vec{k}_{\perp}|$ we finally obtain,

$$(\Pi_{\pm}^{\mu\nu})_B = \left(\frac{g_{\rho\pi\pi}^2}{32\pi^2} \right) \int_0^1 \int_0^1 dx dz z^{\Delta/m_{\pi}^2 - y(1-x)q_{\perp}^2/m_{\pi}^2 - 1} \left(\frac{1}{\tilde{\zeta}} \right) \text{sech}\left(x \frac{eB}{m_{\pi}^2} \ln z\right) \left[\frac{P^{\mu\nu}}{\ln z} + \frac{2Q^{\mu\nu}}{m_{\pi}^2} + \frac{R^{\mu\nu}}{\tilde{\zeta} m_{\pi}^2} \right], \quad (\text{B9})$$

where,

$$P^{\mu\nu} = q^4 g_{\parallel}^{\mu\nu} + q_{\parallel}^2 q^{\mu} q^{\nu} - q^2 (q^{\mu} q_{\parallel}^{\nu} + q^{\nu} q_{\parallel}^{\mu}) \quad (\text{B10})$$

$$Q^{\mu\nu} = q^4 \left[x^2 q_{\parallel}^{\mu} q_{\parallel}^{\nu} + y^2 q_{\perp}^{\mu} q_{\perp}^{\nu} + xy (q_{\parallel}^{\mu} q_{\perp}^{\nu} + q_{\parallel}^{\nu} q_{\perp}^{\mu}) \right] + q^{\mu} q^{\nu} (xq_{\parallel}^2 + yq_{\perp}^2)^2 - q^2 (xq_{\parallel}^2 + yq_{\perp}^2) \left\{ x (q^{\mu} q_{\parallel}^{\nu} + q^{\nu} q_{\parallel}^{\mu}) + y (q^{\mu} q_{\perp}^{\nu} + q^{\nu} q_{\perp}^{\mu}) \right\} \quad (\text{B11})$$

$$R^{\mu\nu} = q^4 g_{\perp}^{\mu\nu} + q_{\perp}^2 q^{\mu} q^{\nu} - q^2 (q^{\mu} q_{\perp}^{\nu} + q^{\nu} q_{\perp}^{\mu}) \quad (\text{B12})$$

In the limit of zero magnetic field, we get back the vacuum self energy as given in Eq. (3), i.e.

$$\lim_{B \rightarrow 0} (\Pi_{\pm}^{\mu\nu})_B = \left(\frac{g_{\rho\pi\pi}^2 q^2}{32\pi^2} \right) (q^2 g^{\mu\nu} - q^{\mu} q^{\nu}) \int_0^1 \int_0^1 dx dz z^{\Delta/m_{\pi}^2 - 1} \frac{m_{\pi}^2}{(\ln z)^2} = (\Pi^{\mu\nu})_{vac}. \quad (\text{B13})$$

Using Eq. (B9) and (B13), we arrive at Eq. (19).

Appendix C: Kinematic Domains of the Imaginary Parts

The imaginary part of the in-medium ρ self energy function at *zero magnetic field* in Eq. (12) contains four Dirac delta functions namely $\delta(q^0 \mp \omega_k \mp \omega_p) = \delta(q^0 \mp E)$ and $\delta(q^0 \mp \omega_k \pm \omega_p) = \delta(q^0 \mp E')$, where $E = \omega_k + \omega_p$ and $E' = \omega_k - \omega_p$. The functions $E = E(|\vec{k}|, \cos\theta)$ and $E' = E'(|\vec{k}|, \cos\theta)$ both are defined in the domain $0 \leq |\vec{k}| < \infty$ and $|\cos\theta| \leq 1$. In this domain the ranges of this two functions are found to be,

$$\sqrt{\bar{q}^2 + 4m_\pi^2} \leq E < \infty \quad \text{and} \quad -|\bar{q}| \leq E' \leq 0 \quad (\text{C1})$$

respectively. So, from Eq. (C1) it is evident that, for $\delta(q^0 - E)$ and $\delta(q^0 + E)$ to be non-vanishing, we must have $\sqrt{\bar{q}^2 + 4m_\pi^2} \leq q^0 < \infty$ and $-\infty < q^0 \leq -\sqrt{\bar{q}^2 + 4m_\pi^2}$ respectively. Similarly for $\delta(q^0 - E')$ and $\delta(q^0 + E')$ to be non-vanishing, we must have $-|\bar{q}| \leq q^0 \leq 0$ and $0 \leq q^0 \leq |\bar{q}|$ respectively.

The imaginary part of the in-medium ρ^0 self energy function at *non-zero magnetic field* in Eq. (18) contains four Dirac delta functions for a particular set of Landau levels $\{n, l\}$ namely $\delta(q^0 \mp \omega_k^l \mp \omega_p^n) = \delta(q^0 \mp E_{n,l})$ and $\delta(q^0 \mp \omega_k^l \pm \omega_p^n) = \delta(q^0 \mp E'_{n,l})$, where $E_{n,l} = \omega_k^l + \omega_p^n$ and $E'_{n,l} = \omega_k^l - \omega_p^n$. The functions $E_{n,l} = E_{n,l}(k_z)$ and $E'_{n,l} = E'_{n,l}(k_z)$ both are defined in the domain $-\infty < k_z < \infty$. In this given domain the ranges of this two functions are found to be,

$$\sqrt{q_z^2 + (m_l + m_n)^2} \leq E_{n,l} < \infty \quad \text{and} \quad \min[q_z, E_{n,l}^\pm] \leq E'_{n,l} \leq \max[q_z, E_{n,l}^\pm] \quad (\text{C2})$$

where, $E_{n,l}^\pm = \frac{(m_l - m_n)}{|m_l \pm m_n|} \sqrt{q_z^2 + (m_l \pm m_n)^2}$. So from Eq. (C2), we find that, for a particular set of Landau levels $\{n, l\}$, for $\delta(q^0 - E_{n,l})$ and $\delta(q^0 + E_{n,l})$ to be non-vanishing, we have $\sqrt{q_z^2 + (m_l + m_n)^2} \leq q^0 < \infty$ and $-\infty < q^0 \leq -\sqrt{q_z^2 + (m_l + m_n)^2}$ respectively. Similarly for $\delta(q^0 - E'_{n,l})$ and $\delta(q^0 + E'_{n,l})$ to be non-vanishing, the corresponding ranges are $\min[q_z, E_{n,l}^\pm] \leq q^0 \leq \max[q_z, E_{n,l}^\pm]$ and $-\max[q_z, E_{n,l}^\pm] \leq q^0 \leq -\min[q_z, E_{n,l}^\pm]$ respectively.

In Eq. (18), the indices l and n run from 0 to ∞ . However for a particular value of l , n can have only three values $l-1, l$ and $l+1$ due to the presence of Kronecker delta function in Eq. (21). Hence, when these indices are summed over from $0 \rightarrow \infty$, $\delta(q^0 - \omega_k^l - \omega_p^n)$ and $\delta(q^0 + \omega_k^l + \omega_p^n)$ will be non-vanishing for $\sqrt{q_z^2 + 4(m_\pi^2 + eB)} < q^0 < \infty$ and $-\infty < q^0 < -\sqrt{q_z^2 + 4(m_\pi^2 + eB)}$ respectively whereas, both $\delta(q^0 - \omega_k^l + \omega_p^n)$ and $\delta(q^0 + \omega_k^l - \omega_p^n)$ will be non-vanishing at $|q^0| < \sqrt{q_z^2 + (\sqrt{m_\pi^2 + eB} - \sqrt{m_\pi^2 + 3eB})^2}$.

Again the imaginary part of the in-medium ρ^\pm self energy function at non-zero magnetic field in Eq. (20) contains four Dirac delta functions for a particular Landau level n namely $\delta(q^0 \mp \omega_k \mp \omega_p^n) = \delta(q^0 \mp E_n)$ and $\delta(q^0 \mp \omega_k \pm \omega_p^n) = \delta(q^0 \mp E'_n)$, where $E_n = \omega_k + \omega_p^n$ and $E'_n = \omega_k - \omega_p^n$. The functions $E_n = E_n(|\vec{k}|, \cos\theta)$ and $E'_n = E'_n(|\vec{k}|, \cos\theta)$ both are defined in the domain $0 \leq |\vec{k}| < \infty$ and $|\cos\theta| \leq 1$. In this domain the ranges of these two functions are found to be,

$$\sqrt{q_z^2 + (m_\pi + m_n)^2} \leq E_n < \infty \quad \text{and} \quad -\sqrt{q_z^2 + (m_\pi - m_n)^2} \leq E'_n \leq 0 \quad (\text{C3})$$

respectively. So from Eq. (C3), we find that, for a particular Landau level n , for $\delta(q^0 - E_n)$ and $\delta(q^0 + E_n)$ to be non-zero, q^0 must lie in the range $\sqrt{q_z^2 + (m_\pi + m_n)^2} \leq q^0 < \infty$ and $-\infty < q^0 \leq -\sqrt{q_z^2 + (m_\pi + m_n)^2}$ respectively. Similarly, for $\delta(q^0 - E'_n)$ and $\delta(q^0 + E'_n)$ to be non-vanishing, the inequalities $-\sqrt{q_z^2 + (m_\pi - m_n)^2} \leq q^0 \leq 0$ and $0 \leq q^0 \leq \sqrt{q_z^2 + (m_\pi - m_n)^2}$ must be satisfied.

In Eq. (20), the index n runs from 0 to ∞ and when it is summed over, $\delta(q^0 - \omega_k - \omega_p^n)$ and $\delta(q^0 + \omega_k + \omega_p^n)$ will be non-vanishing at $\sqrt{q_z^2 + (\sqrt{m_\pi^2 + eB} + m_\pi)^2} < q^0 < \infty$ and $-\infty < q^0 < -\sqrt{q_z^2 + (\sqrt{m_\pi^2 + eB} + m_\pi)^2}$ respectively whereas, $\delta(q^0 - \omega_k + \omega_p^n)$ and $\delta(q^0 + \omega_k - \omega_p^n)$ will be non-vanishing at $0 < q^0 < \infty$ and $-\infty < q^0 < 0$ respectively.

Appendix D: Simplification of the Imaginary Parts

The imaginary part of in-medium self energy function of ρ at *zero magnetic field* in Eq. (12) can be written as,

$$\begin{aligned} \text{Im } \bar{\Pi}^{\mu\nu}(q) = & -\pi\epsilon(q^0) \int_0^\infty \int_0^\pi \int_0^{2\pi} \frac{|\vec{k}|^2 \sin\theta d|\vec{k}| d\theta d\phi}{(2\pi)^3 4\omega_k \omega_p} \left[U_1(q, \vec{k}) \delta(q^0 - \omega_k - \omega_p) + U_2(q, \vec{k}) \delta(q^0 + \omega_k + \omega_p) \right. \\ & \left. + L_1(q, \vec{k}) \delta(q^0 + \omega_k - \omega_p) + L_2(q, \vec{k}) \delta(q^0 - \omega_k + \omega_p) \right], \end{aligned} \quad (\text{D1})$$

where,

$$\begin{aligned} U_1 &= (1 + \eta^k + \eta^p) \mathcal{N}^{\mu\nu}(q, k^0 = \omega_k, \vec{k}) \\ U_2 &= (-1 - \eta^k - \eta^p) \mathcal{N}^{\mu\nu}(q, k^0 = -\omega_k, \vec{k}) \\ L_1 &= (\eta^k - \eta^p) \mathcal{N}^{\mu\nu}(q, k^0 = -\omega_k, \vec{k}) \\ L_2 &= (-\eta^k + \eta^p) \mathcal{N}^{\mu\nu}(q, k^0 = \omega_k, \vec{k}) \end{aligned}$$

For simplicity, we have taken $\vec{q} = \vec{0}$ and it is to be noted that, the nonzero components of $\mathcal{N}^{\mu\nu}(q^0, \vec{q} = \vec{0}, \vec{k})$ are independent of θ and ϕ . In Appendix (C) it is shown that, for $\vec{q} = \vec{0}$ only Unitary terms contribute. So Eq. (D1) simplifies to,

$$\begin{aligned} \text{Im } \bar{\Pi}^{\mu\nu}(q^0) = & \frac{-\epsilon(q^0)}{8\pi} \int_0^\infty \frac{|\vec{k}|^2 d|\vec{k}|}{\omega_k^2} \left[U_1(q^0, |\vec{k}|) \delta(q^0 - 2\omega_k) \Theta(q^0 - 2m_\pi) \right. \\ & \left. + U_2(q^0, |\vec{k}|) \delta(q^0 + 2\omega_k) \Theta(-q^0 - 2m_\pi) \right]. \end{aligned}$$

Transforming the Dirac delta functions $\delta(q^0 \mp 2\omega_k) = \left(\frac{\omega_k}{2|\vec{k}|}\right) \delta(|\vec{k}| - \tilde{k})$ where $\tilde{k} = \left(\frac{1}{2q^0}\right) \lambda^{1/2}(q_0^2, m_\pi^2, m_\pi^2)$ and performing the remaining $|\vec{k}|$ integration we arrive at Eq. (22). Here $\Theta(x)$ is the unit step function and $\lambda(x, y, z) = (x^2 + y^2 + z^2 - 2xy - 2yz - 2zx)$ is the Kallen function.

We now turn on the magnetic field. The imaginary part of in-medium self energy function of ρ^0 at *non-zero magnetic field* in Eq. (18) for $\vec{q} = \vec{0}$ can be written as,

$$\begin{aligned} \text{Im } \bar{\Pi}_0^{\mu\nu} = & -\pi\epsilon(q^0) \sum_{l=0}^\infty \sum_{n=0}^\infty \int_{-\infty}^{+\infty} \frac{dk_z}{(2\pi)} \frac{1}{4\omega_k^l \omega_k^n} \left[U_1^{n,l}(q^0, k_z) \delta(q^0 - \omega_k^l - \omega_k^n) + U_2^{n,l}(q^0, k_z) \delta(q^0 + \omega_k^l + \omega_k^n) \right. \\ & \left. + L_1^{n,l}(q^0, k_z) \delta(q^0 + \omega_k^l - \omega_k^n) + L_2^{n,l}(q^0, k_z) \delta(q^0 - \omega_k^l + \omega_k^n) \right] \end{aligned}$$

where,

$$\begin{aligned} U_1^{n,l} &= (1 + \eta_l^k + \eta_n^k) \mathcal{N}_{n,l}^{\mu\nu}(q, k^0 = \omega_k^l, k_z) \\ U_2^{n,l} &= (-1 - \eta_l^k - \eta_n^k) \mathcal{N}_{n,l}^{\mu\nu}(q, k^0 = -\omega_k^l, k_z) \\ L_1^{n,l} &= (\eta_l^k - \eta_n^k) \mathcal{N}_{n,l}^{\mu\nu}(q, k^0 = -\omega_k^l, k_z) \\ L_2^{n,l} &= (-\eta_l^k + \eta_n^k) \mathcal{N}_{n,l}^{\mu\nu}(q, k^0 = \omega_k^l, k_z) \end{aligned}$$

Now we transform the Dirac delta functions $\delta(q^0 \mp \omega_k^l \mp \omega_k^n) = \delta(q^0 \mp \omega_k^l \pm \omega_k^n) = \left(\frac{\omega_k^l \omega_k^n}{|k_z q^0|}\right) \left[\delta(k_z - \tilde{k}_z) + \delta(k_z + \tilde{k}_z)\right]$ where $\tilde{k}_z = \left(\frac{1}{2q^0}\right) \lambda^{1/2}(q_0^2, m_l^2, m_n^2)$ and impose the kinematic domains as obtained in Appendix (C). After performing the k_z integration we arrive at Eq. (23).

We now look at the charged ρ . The imaginary part of in-medium self energy function of ρ^\pm at *non-zero magnetic field* in Eq. (20) for $\vec{q} = (q_x, q_y, 0)$ can be written as,

$$\begin{aligned} \text{Im } \bar{\Pi}_\pm^{\mu\nu} = & -\pi\epsilon(q^0) \sum_{n=0}^{\infty} \int_0^{\infty} \int_0^{\pi} \int_0^{2\pi} \frac{|\vec{k}|^2 \sin\theta d\theta d\phi}{(2\pi)^3} \frac{1}{4\omega_k \omega_k^n} \left[U_1^n(q^0, \vec{k}) \delta(q^0 - \omega_k - \omega_k^n) + U_2^n(q^0, \vec{k}) \delta(q^0 + \omega_k + \omega_k^n) \right. \\ & \left. + L_1^n(q^0, \vec{k}) \delta(q^0 + \omega_k - \omega_k^n) + L_2^n(q^0, \vec{k}) \delta(q^0 - \omega_k + \omega_k^n) \right] \end{aligned} \quad (\text{D2})$$

where,

$$\begin{aligned} U_1^n &= \phi_n(\alpha_k) (1 + \eta^k + \eta_n^k) \mathcal{N}^{\mu\nu}(q, k^0 = \omega_k, \vec{k}) \\ U_2^n &= \phi_n(\alpha_k) (-1 - \eta^k - \eta_n^k) \mathcal{N}^{\mu\nu}(q, k^0 = -\omega_k, \vec{k}) \\ L_1^n &= \phi_n(\alpha_k) (\eta^k - \eta_n^k) \mathcal{N}^{\mu\nu}(q, k^0 = -\omega_k, \vec{k}) \\ L_2^n &= \phi_n(\alpha_k) (-\eta^k + \eta_n^k) \mathcal{N}^{\mu\nu}(q, k^0 = \omega_k, \vec{k}) \end{aligned}$$

Now we write the Dirac delta functions as,

$$\begin{aligned} \delta(q^0 - \omega_k \mp \omega_k^n) &= \left(\frac{\omega_k^n}{|\vec{k}|^2 \cos\theta_0} \right) \left[\delta(\cos\theta - \cos\theta_0) + \delta(\cos\theta + \cos\theta_0) \right] \\ \delta(q^0 + \omega_k \mp \omega_k^n) &= \left(\frac{\omega_k^n}{|\vec{k}|^2 \cos\theta'_0} \right) \left[\delta(\cos\theta - \cos\theta'_0) + \delta(\cos\theta + \cos\theta'_0) \right] \end{aligned} \quad (\text{D3})$$

where $\cos\theta_0 = \frac{1}{|\vec{k}|} \sqrt{(q^0 + \omega_k)^2 - m_n^2}$ and $\cos\theta'_0 = \frac{1}{|\vec{k}|} \sqrt{(q^0 - \omega_k)^2 - m_n^2}$. Changing the variable of integration from $|\vec{k}|$ to ω_k and performing the θ integration using the transformed Dirac delta function and imposing the kinematic domains as obtained in Appendix (C), Eq. (D2) becomes,

$$\begin{aligned} \text{Im } \bar{\Pi}_\pm^{\mu\nu} = & \frac{-\epsilon(q^0)}{32\pi^2} \sum_{n=0}^{\infty} \int_{m_\pi}^{\infty} \frac{d\omega_k}{|\vec{k}|} \int_0^{2\pi} d\phi \left[\frac{\Theta(1 - \cos\theta_0)}{\cos\theta_0} \left\{ U_1^n(q^0, |\vec{k}|, \theta_0, \phi) + U_1^n(q^0, |\vec{k}|, -\theta_0, \phi) \right\} \Theta(q^0 - m_\pi - m_n) \right. \\ & + \frac{\Theta(1 - \cos\theta'_0)}{\cos\theta'_0} \left\{ U_2^n(q^0, |\vec{k}|, \theta'_0, \phi) + U_2^n(q^0, |\vec{k}|, -\theta'_0, \phi) \right\} \Theta(-q^0 - m_\pi - m_n) \\ & + \frac{\Theta(1 - \cos\theta'_0)}{\cos\theta'_0} \left\{ L_1^n(q^0, |\vec{k}|, \theta'_0, \phi) + L_1^n(q^0, |\vec{k}|, -\theta'_0, \phi) \right\} \Theta(-q^0 - m_\pi + m_n) \Theta(q^0) \\ & \left. + \frac{\Theta(1 - \cos\theta_0)}{\cos\theta_0} \left\{ L_2^n(q^0, |\vec{k}|, \theta_0, \phi) + L_2^n(q^0, |\vec{k}|, -\theta_0, \phi) \right\} \Theta(q^0 - m_\pi + m_n) \Theta(-q^0) \right]. \end{aligned} \quad (\text{D4})$$

In Eq. (D4), the presence of the $\Theta(1 - \cos\theta_0)$ and $\Theta(1 - \cos\theta'_0)$ will further put restriction on the limits of the ω_k integration and we will get Eq. (24).

-
- [1] D. E. Kharzeev, K. Landsteiner, A. Schmitt and H. U. Yee, Lect. Notes Phys. **871**, 1 (2013) [arXiv:1211.6245 [hep-ph]].
[2] D. Kharzeev and A. Zhitnitsky, Nucl. Phys. A **797**, 67 (2007) [arXiv:0706.1026 [hep-ph]].
[3] D. E. Kharzeev, L. D. McLerran and H. J. Warringa, Nucl. Phys. A **803**, 227 (2008) [arXiv:0711.0950 [hep-ph]].
[4] K. Fukushima, D. E. Kharzeev and H. J. Warringa, Phys. Rev. D **78**, 074033 (2008) [arXiv:0808.3382 [hep-ph]].
[5] V. P. Gusynin, V. A. Miransky and I. A. Shovkovy, Nucl. Phys. B **462**, 249 (1996) [hep-ph/9509320].
[6] V. P. Gusynin, V. A. Miransky and I. A. Shovkovy, Nucl. Phys. B **563**, 361 (1999) [hep-ph/9908320].
[7] G. S. Bali, F. Bruckmann, G. Endrodi, Z. Fodor, S. D. Katz, S. Krieg, A. Schafer and K. K. Szabo, JHEP **1202**, 044 (2012) [arXiv:1111.4956 [hep-lat]].
[8] M. N. Chernodub, Phys. Rev. D **82**, 085011 (2010) [arXiv:1008.1055 [hep-ph]].

- [9] M. N. Chernodub, Lect. Notes Phys. **871**, 143 (2013) [arXiv:1208.5025 [hep-ph]].
- [10] V. Skokov, A. Y. Illarionov and V. Toneev, Int. J. Mod. Phys. A **24**, 5925 (2009) [arXiv:0907.1396 [nucl-th]].
- [11] R. C. Duncan and C. Thompson, Astrophys. J. **392**, L9 (1992).
- [12] E. J. Ferrer, V. de la Incera and C. Manuel, Phys. Rev. Lett. **95**, 152002 (2005) [hep-ph/0503162].
- [13] E. J. Ferrer, V. de la Incera and C. Manuel, Nucl. Phys. B **747**, 88 (2006) [hep-ph/0603233].
- [14] E. J. Ferrer and V. de la Incera, Phys. Rev. D **76**, 045011 (2007) [nucl-th/0703034 [NUCL-TH]].
- [15] K. Fukushima and H. J. Warringa, Phys. Rev. Lett. **100**, 032007 (2008) [arXiv:0707.3785 [hep-ph]].
- [16] B. Feng, D. Hou, H. c. Ren and P. p. Wu, Phys. Rev. Lett. **105**, 042001 (2010) [arXiv:0911.4997 [hep-ph]].
- [17] S. Fayazbakhsh and N. Sadooghi, Phys. Rev. D **82**, 045010 (2010) [arXiv:1005.5022 [hep-ph]].
- [18] S. Fayazbakhsh and N. Sadooghi, Phys. Rev. D **83**, 025026 (2011) [arXiv:1009.6125 [hep-ph]].
- [19] J. O. Andersen, W. R. Naylor and A. Tranberg, Rev. Mod. Phys. **88**, 025001 (2016) [arXiv:1411.7176 [hep-ph]].
- [20] K. I. Wang, S. x. Qin, Y. x. Liu, L. Chang, C. D. Roberts and S. M. Schmidt, Phys. Rev. D **86**, 114001 (2012) [arXiv:1209.2757 [nucl-th]].
- [21] C. Vafa and E. Witten, Nucl. Phys. B **234**, 173 (1984).
- [22] Y. Hidaka and A. Yamamoto, Phys. Rev. D **87**, no. 9, 094502 (2013) [arXiv:1209.0007 [hep-ph]].
- [23] M. N. Chernodub, Phys. Rev. D **86**, 107703 (2012) [arXiv:1209.3587 [hep-ph]].
- [24] C. Li and Q. Wang, Phys. Lett. B **721**, 141 (2013) [arXiv:1301.7009 [hep-th]].
- [25] M. N. Chernodub, Phys. Rev. D **89**, no. 1, 018501 (2014) [arXiv:1309.4071 [hep-ph]].
- [26] H. Liu, L. Yu and M. Huang, Phys. Rev. D **91**, no. 1, 014017 (2015) [arXiv:1408.1318 [hep-ph]].
- [27] M. Kawaguchi and S. Matsuzaki, Phys. Rev. D **93**, no. 12, 125027 (2016) [arXiv:1511.06990 [hep-ph]].
- [28] R. Rapp and J. Wambach, Adv. Nucl. Phys. **25**, 1 (2000) [hep-ph/9909229].
- [29] J. Alam, S. Sarkar, P. Roy, T. Hatsuda and B. Sinha, Annals Phys. **286**, 159 (2001) [hep-ph/9909267].
- [30] S. Mallik and S. Sarkar, *“Hadrons at Finite Temperature,”* Cambridge University Press.
- [31] S. Ghosh, S. Sarkar and S. Mallik, Eur. Phys. J. C **70**, 251 (2010) [arXiv:0911.3504 [hep-ph]].
- [32] S. Ghosh, A. Mukherjee, M. Mandal, S. Sarkar and P. Roy, Phys. Rev. D **94** 094043.
- [33] J. Navarro, A. Sanchez, M. E. Tejeda-Yeomans, A. Ayala and G. Piccinelli, Phys. Rev. D **82**, 123007 (2010) [arXiv:1007.4208 [hep-ph]].
- [34] A. Ayala, A. Sanchez, G. Piccinelli and S. Sahu, Phys. Rev. D **71**, 023004 (2005) [hep-ph/0412135].
- [35] A. Bandyopadhyay, C. A. Islam and M. G. Mustafa, Phys. Rev. D **94**, 114034 (2016) [arXiv:1602.06769 [hep-ph]].
- [36] J. C. D’Olivo, J. F. Nieves and S. Sahu, Phys. Rev. D **67**, 025018 (2003) [hep-ph/0208146].
- [37] K. Hattori and K. Itakura, Annals Phys. **330**, 23 (2013) [arXiv:1209.2663 [hep-ph]].
- [38] M. Le Bellac, *“Thermal Field Theory,”* Cambridge University Press, Cambridge, England, 1996.
- [39] J. S. Schwinger, Phys. Rev. **82**, 664 (1951).
- [40] A. Ayala, C. A. Dominguez, L. A. Hernandez, M. Loewe, J. C. Rojas and C. Villavicencio, Phys. Rev. D **92**, no. 1, 016006 (2015) [arXiv:1504.01308 [hep-ph]].
- [41] M. D. Schwartz, *“Quantum Field Theory and the Standard Model,”* Cambridge University Press.